

Lecture 2: Neutrino interactions and their measurements

PhD, XXXIV Cycle

Topic

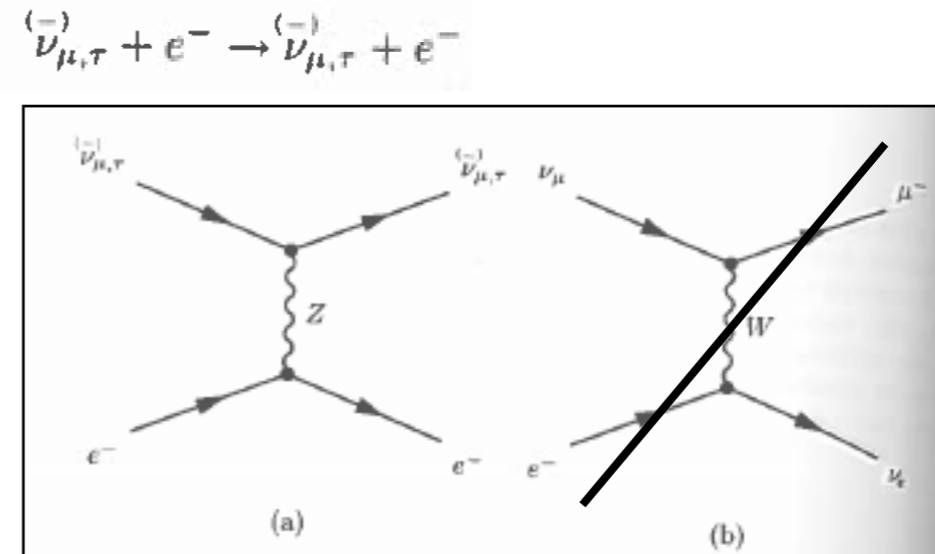
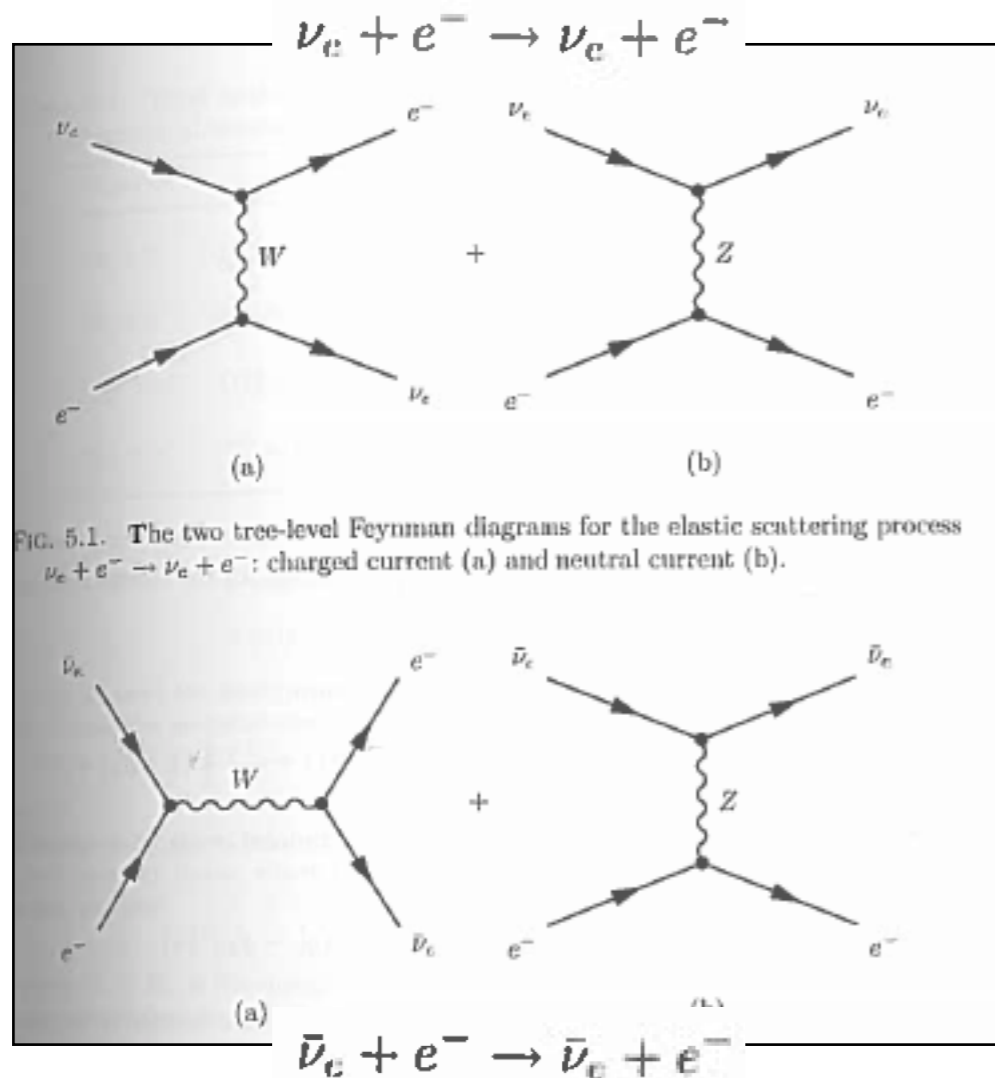
- Neutrino physics experiments have to make do with **indirect** detection of ν via their interaction with the detector
- ν and $\bar{\nu}$ interact both with leptons and nucleons
- let's see how -- an **overview!**
- what sub-processes matter in the current experiments?
 - important effects on “fundamental” measurements (e.g. oscillations), translate into systematic uncertainties
 - special focus on “auxiliary” measures like those from MiniBoone, MINERvA, T2K in constraining the different contributions

ν - e interactions

Low-energy neutrinos and antineutrinos with flavor $\alpha = e, \mu, \tau$ interact with electrons through the elastic scattering process

$$\nu_{\alpha}^{(-)} + e^{-} \rightarrow \nu_{\alpha}^{(-)} + e^{-} \quad (5.5)$$

This process is used, for example, in water Cherenkov solar neutrino detectors (see section 10.6). The elastic scattering process does not have a threshold, since the final state is the same as the initial state. The only effect of an elastic scattering process is a redistribution of the total energy and momentum between the two participating particles.



see later

ν - e relative occurrences (in the void)

TABLE 5.1. Total neutrino–electron elastic scattering cross-sections for $\sqrt{s} \gg m_e$. The numerical values are in units of 10^{-16} cm^2 .

Process	Total cross-section
$\nu_e + e^-$	$(G_F^2 s/4\pi) \left[(1 + 2 \sin^2 \vartheta_W)^2 + \frac{4}{3} \sin^4 \vartheta_W \right] \simeq 93 \text{ s/MeV}^2$
$\bar{\nu}_e + e^-$	$(G_F^2 s/4\pi) \left[\frac{1}{3} (1 + 2 \sin^2 \vartheta_W)^2 + 4 \sin^4 \vartheta_W \right] \simeq 39 \text{ s/MeV}^2$
$\nu_{\mu,\tau} + e^-$	$(G_F^2 s/4\pi) \left[(1 - 2 \sin^2 \vartheta_W)^2 + \frac{4}{3} \sin^4 \vartheta_W \right] \simeq 15 \text{ s/MeV}^2$
$\bar{\nu}_{\mu,\tau} + e^-$	$(G_F^2 s/4\pi) \left[\frac{1}{3} (1 - 2 \sin^2 \vartheta_W)^2 + 4 \sin^4 \vartheta_W \right] \simeq 13 \text{ s/MeV}^2$

Fundamentals of Neutrino Physics and Astrophysics

by: Carlo Giunti and Chung W. Kim, Oxford UP 2007

for $\sqrt{s} \gg m_e$ the approximate ratios of the four cross-sections are

$$\sigma_{\nu_e} : \sigma_{\bar{\nu}_e} : \sigma_{\nu_{\mu,\tau}} : \sigma_{\bar{\nu}_{\mu,\tau}} \simeq 1 : 0.42 : 0.16 : 0.14. \quad (5.18)$$

$\sigma \approx 10^{-44} \text{ cm}^2$ Mean free path: $\lambda = \frac{1}{n\sigma} \approx 1.5 \times 10^{21} \text{ cm} \approx 1600 \text{ light-years}$

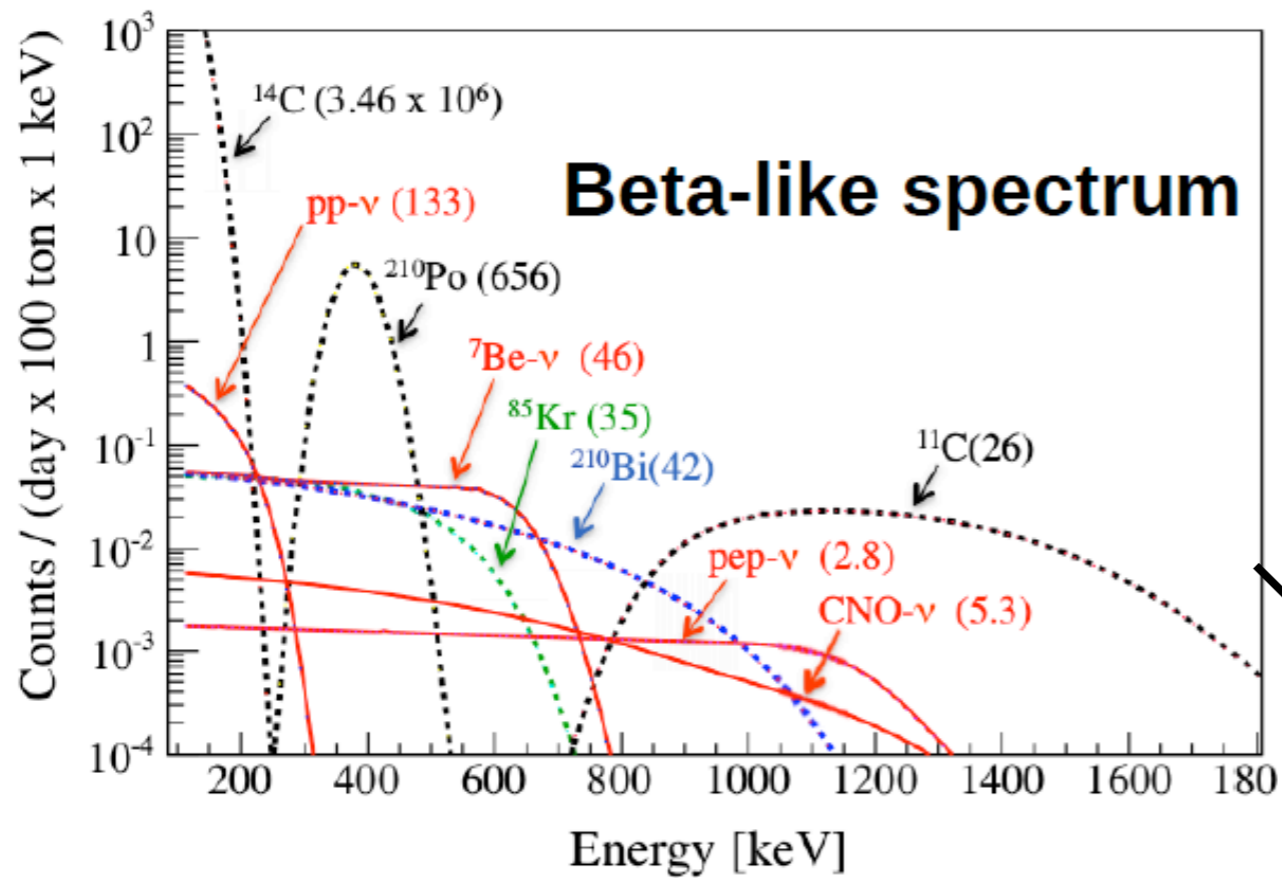
$n = \frac{\text{num. free protons}}{\text{volume}} \approx 2 \frac{N_A}{A} \rho$ In water: $n = \frac{2 \times 6 \times 10^{23}}{18} = 6.7 \times 10^{22} \text{ cm}^{-3}$

Example

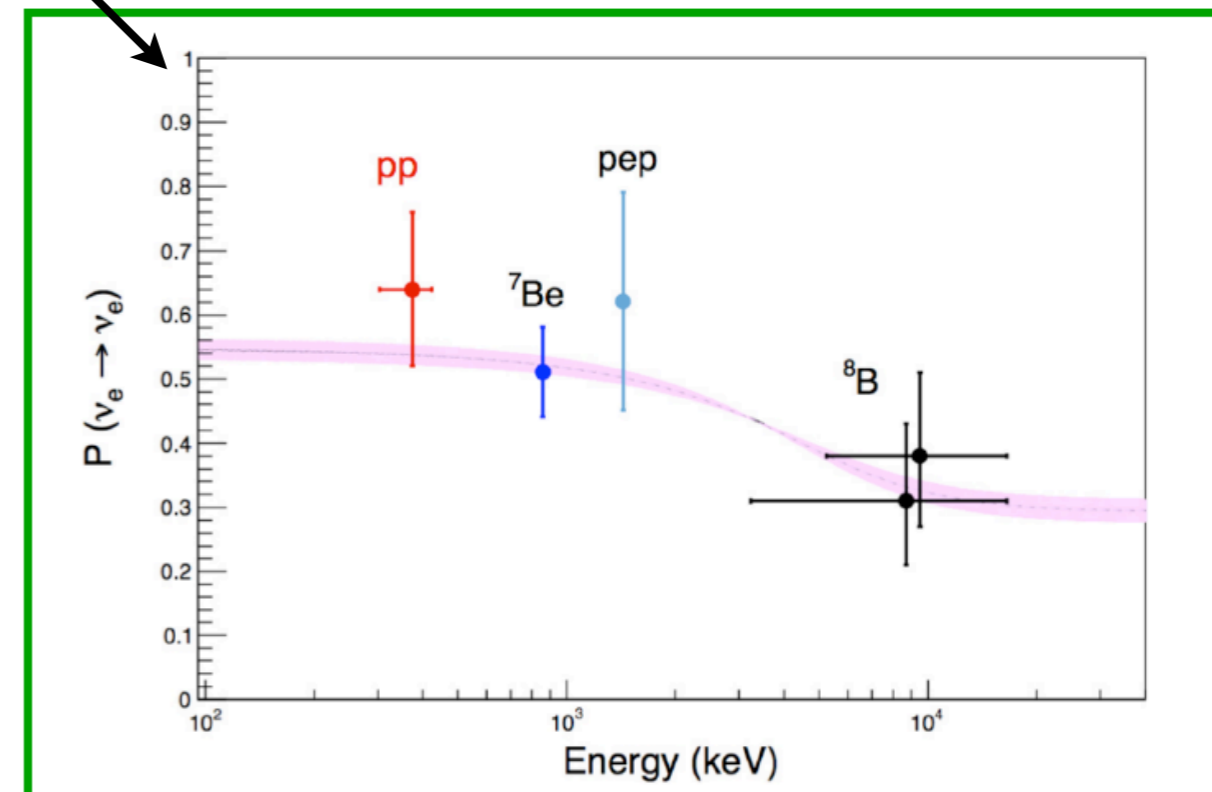
ν - e relative occurrences (**experiments**)

Crucial point:
Extreme low background required!!!

Example



Solar neutrinos at Borexino
Low energy threshold thanks to very low
radio-active bkg
But anyway only one integrated point per
species,
BOREXINO has effective threshold ~ 200
keV



ν - e relative occurrences (experiments)

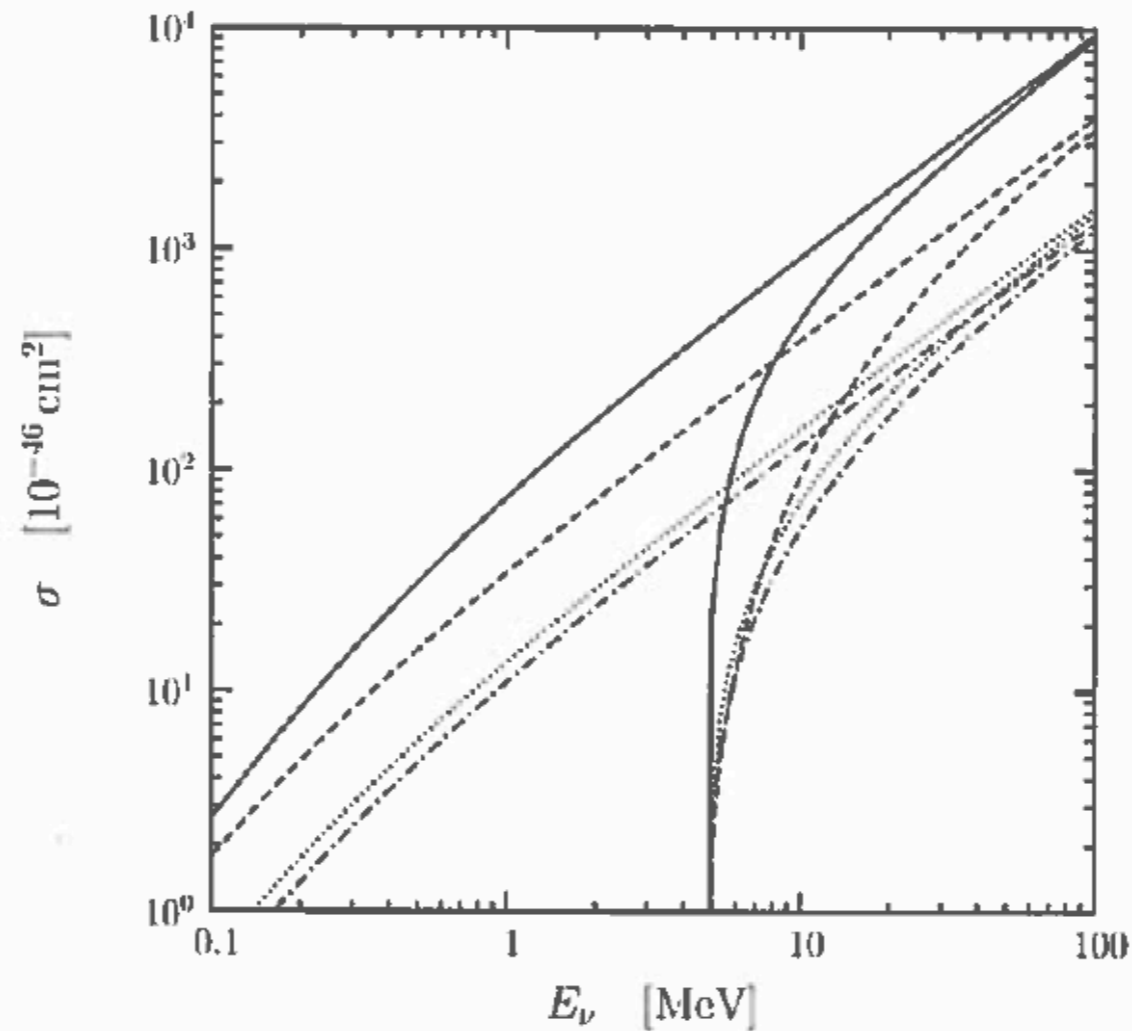


FIG. 5.5. Neutrino-electron cross-sections in eqn (5.32) as functions of the neutrino energy E_ν . Solid line: $\nu_e + e^- \rightarrow \nu_e + e^-$. Dashed line: $\bar{\nu}_e + e^- \rightarrow \bar{\nu}_e + e^-$. Dotted line: $\nu_{\mu,\tau} + e^- \rightarrow \nu_{\mu,\tau} + e^-$. Dash-dotted line: $\bar{\nu}_{\mu,\tau} + e^- \rightarrow \bar{\nu}_{\mu,\tau} + e^-$. For each scattering process the upper curve is the cross-section without a threshold for the kinetic energy of the recoil electron, whereas the lower curve is obtained with $T_e^{\text{th}} = 4.50 \text{ MeV}$, which corresponds to $E_\nu^{\text{th}} = 4.74 \text{ MeV}$, according to eqn (5.31).

- At very low energies, cannot distinguish relevant neutrino signals from experimental backgrounds
- There is always a threshold below which a measurement is not performed

ν - ℓ and ν - \mathcal{N} relative occurrences (void)

Muon neutrinos with energy above the μ production threshold can interact with electrons through the quasielastic charged-current process

$$\nu_\mu + e^- \rightarrow \nu_e + \mu^- \quad (5.35)$$

TABLE 5.2. Threshold neutrino energy in eqn (5.37) for some charged-current reactions used for neutrino detection.

Reaction	Masses	E_ν^{th}
$\nu_e + {}^{71}\text{Ga} \rightarrow {}^{71}\text{Ge} + e^-$	$m({}^{71}\text{Ga}) = 66050.093 \text{ MeV}$ $m({}^{71}\text{Ge}) = 66049.814 \text{ MeV}$	0.23 MeV
$\nu_e + {}^{37}\text{Cl} \rightarrow {}^{37}\text{Ar} + e^-$	$m({}^{37}\text{Cl}) = 34424.829 \text{ MeV}$ $m({}^{37}\text{Ar}) = 34425.132 \text{ MeV}$	0.82 MeV
$\bar{\nu}_e + p \rightarrow n + e^+$	$m_p = 938.272 \text{ MeV}$ $m_n = 939.565 \text{ MeV}$	1.81 MeV
$\nu + d \rightarrow p + n + \nu$	$m_d = 1875.613 \text{ MeV}$	2.23 MeV
$\nu_\mu + n \rightarrow p + \mu^-$	$m_\mu = 105.658 \text{ MeV}$	110.16 MeV
$\nu_\tau + n \rightarrow p + \tau^-$	$m_\tau = 1777.03 \text{ MeV}$	3.45 GeV
$\nu_\mu + e^- \rightarrow \mu^- + \nu_e$	$m_e = 0.511 \text{ MeV}$	10.92 GeV

solar (elastic) \rightarrow

reactors (elastic IBD) \rightarrow

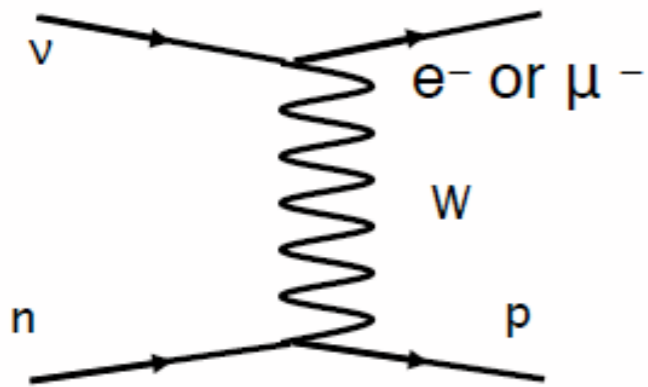
disappearance (quasi-elastic) \rightarrow

$$\nu + A \rightarrow \sum_X X$$

$$E_\nu^{\text{th}} = \frac{(\sum_X m_X)^2}{2m_A} - \frac{m_A}{2}$$

ν -N interactions: problems arise

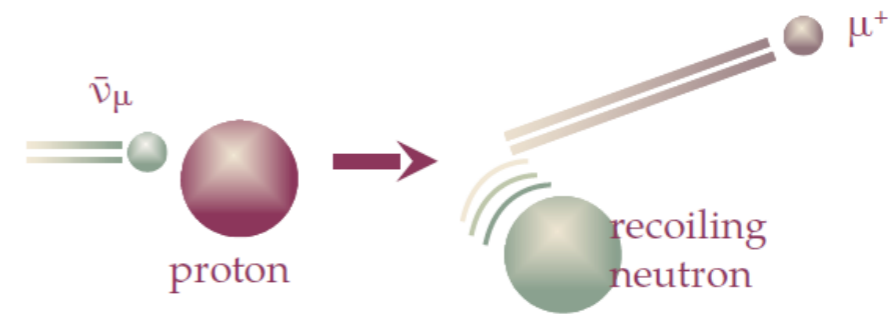
Charged-Current Quasi-Elastic (CCQE)



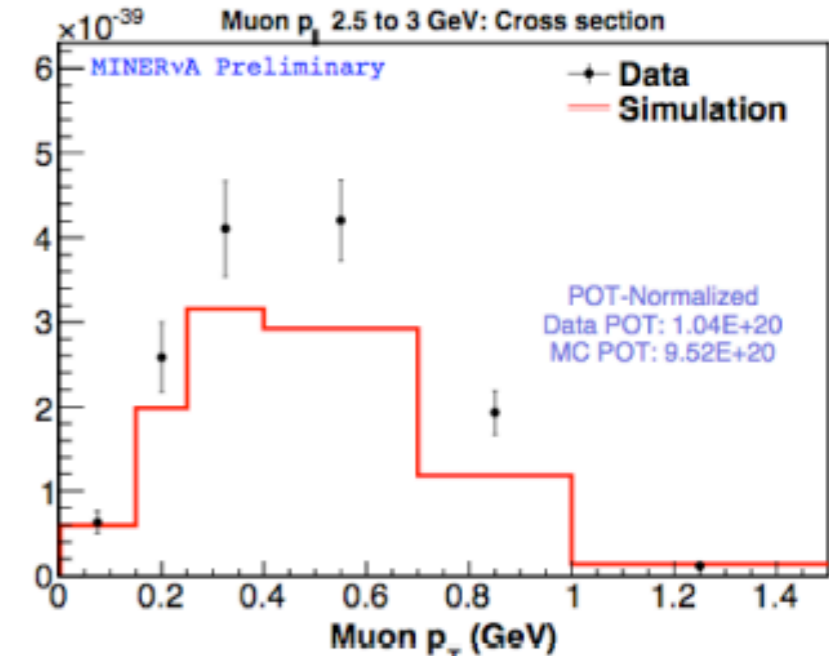
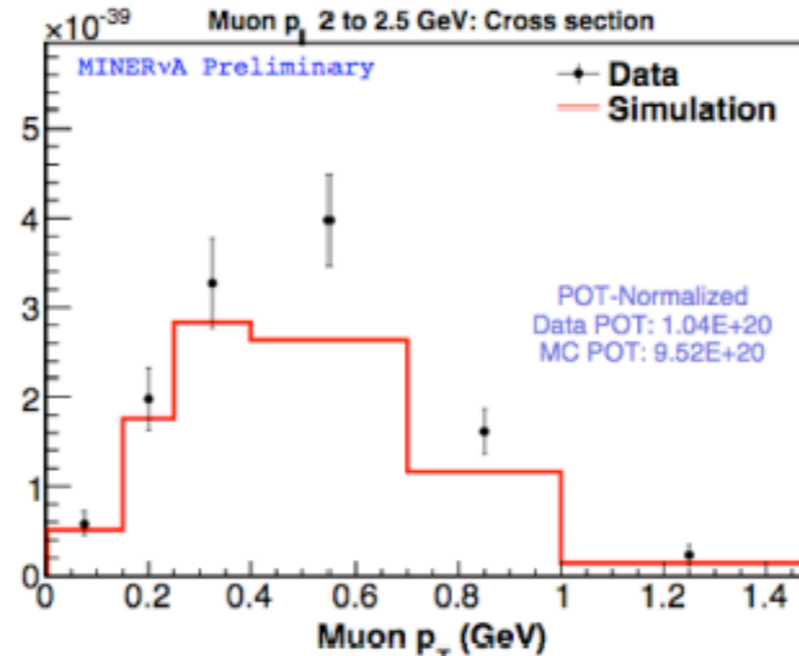
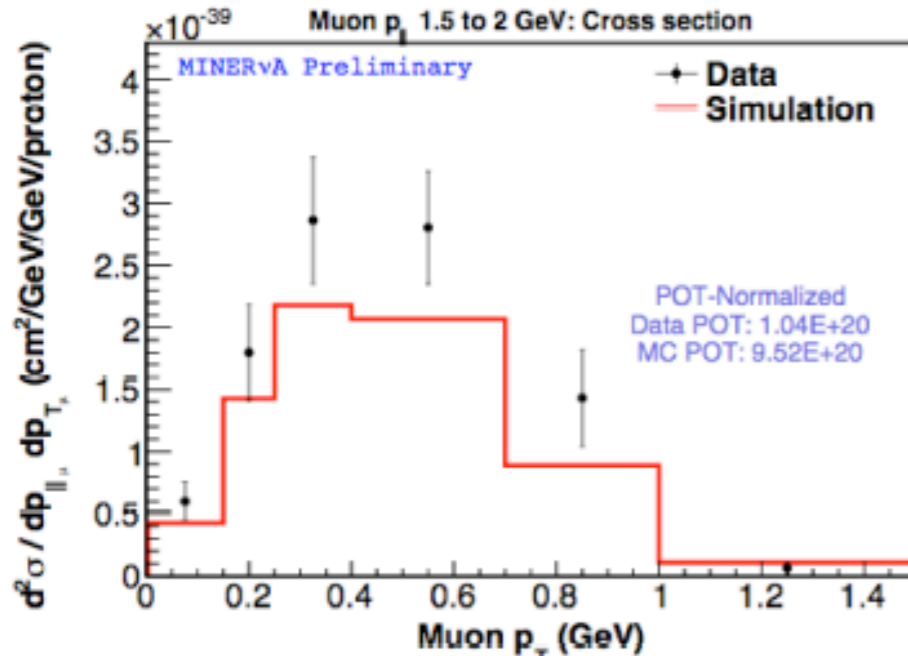
Theory: relatively well understood (same as e -N scattering)

Experiments

QE-like = 0 pions



Excesses!



..but e-N(p or n) OK

$$\frac{d^2\sigma_{IA}}{d\Omega_{e'}dE_{e'}} = \int d^3k dE P(\mathbf{k}, E) \quad (22)$$

$$\times \left[Z \frac{d^2\sigma_{ep}}{d\Omega_{e'}dE_{e'}} + N \frac{d^2\sigma_{en}}{d\Omega_{e'}dE_{e'}} \right],$$

with

$$\frac{d^2\sigma_{e\alpha}}{d\Omega_{e'}dE_{e'}} = \frac{\alpha^2}{Q^4} \frac{E_{e'}}{E_e} L_{\mu\nu} \mathcal{W}_\alpha^{\mu\nu}. \quad (23)$$

Impulse Approximation scheme

$\mathbf{q}^{-1} \ll 2\pi/d$, d being the average distance between nucleons in the target nucleus, the nuclear scattering process reduces to an incoherent sum of collisions involving individual nucleons, as illustrated in Fig. 4, the remaining $A - 1$ particles acting as spectators. Moreover, final

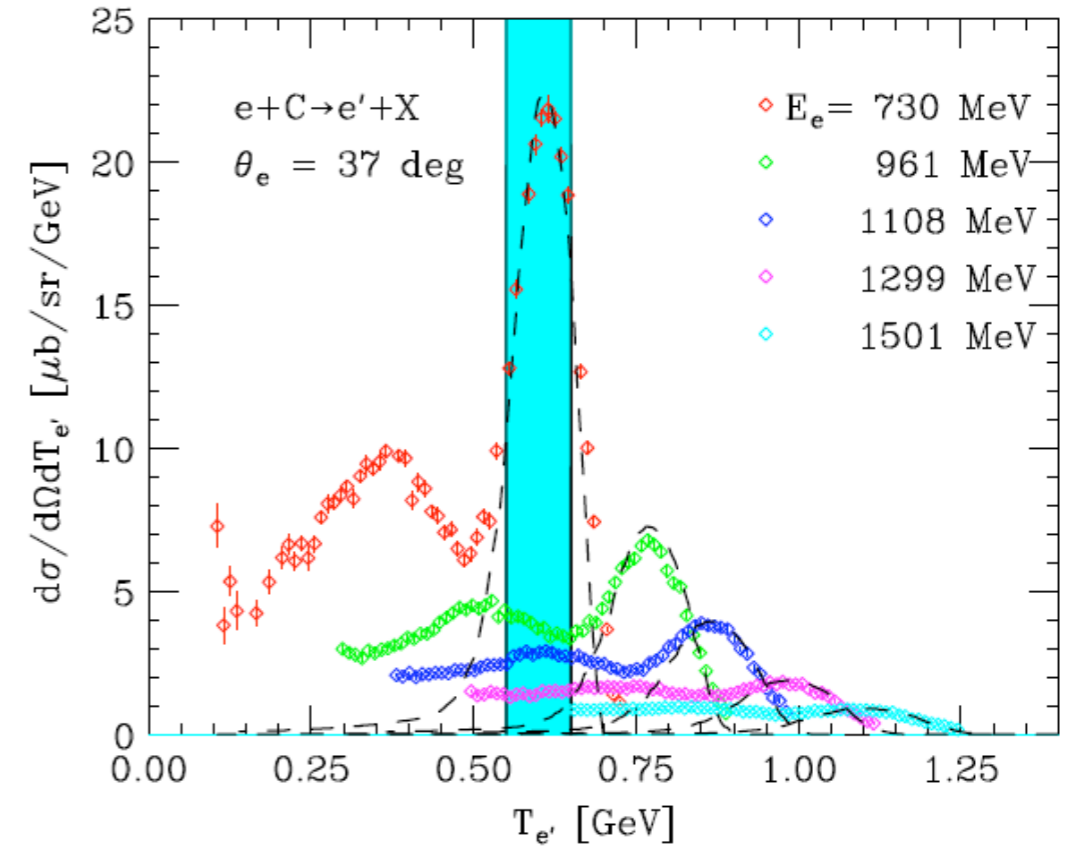


FIG. 2 (color online) Inclusive electron-carbon cross sections at $\theta_e = 37$ deg and beam energies ranging between 0.730 and 1.501 GeV (O'Connell *et al.*, 1987; Sealock *et al.*, 1989), plotted as a function of the energy of the outgoing electron (Benhar and Rocco, 2013). The dashed lines represent the results of theoretical calculations, carried out taking into account QE scattering only.

Then what's wrong with ν -N?

$$\nu_\ell + A \rightarrow \ell^- + X, \quad \frac{d^2\sigma}{d\Omega_\ell dE_\ell} = \frac{G_F^2 V_{ud}^2}{16\pi^2} \frac{|\mathbf{k}_\ell|}{|\mathbf{k}_\nu|} L_{\lambda\mu} W^{\lambda\mu}.$$

An **effective “quasi-elastic”** treatment with 1 nucleon interaction, merely adding the axial current for neutrinos

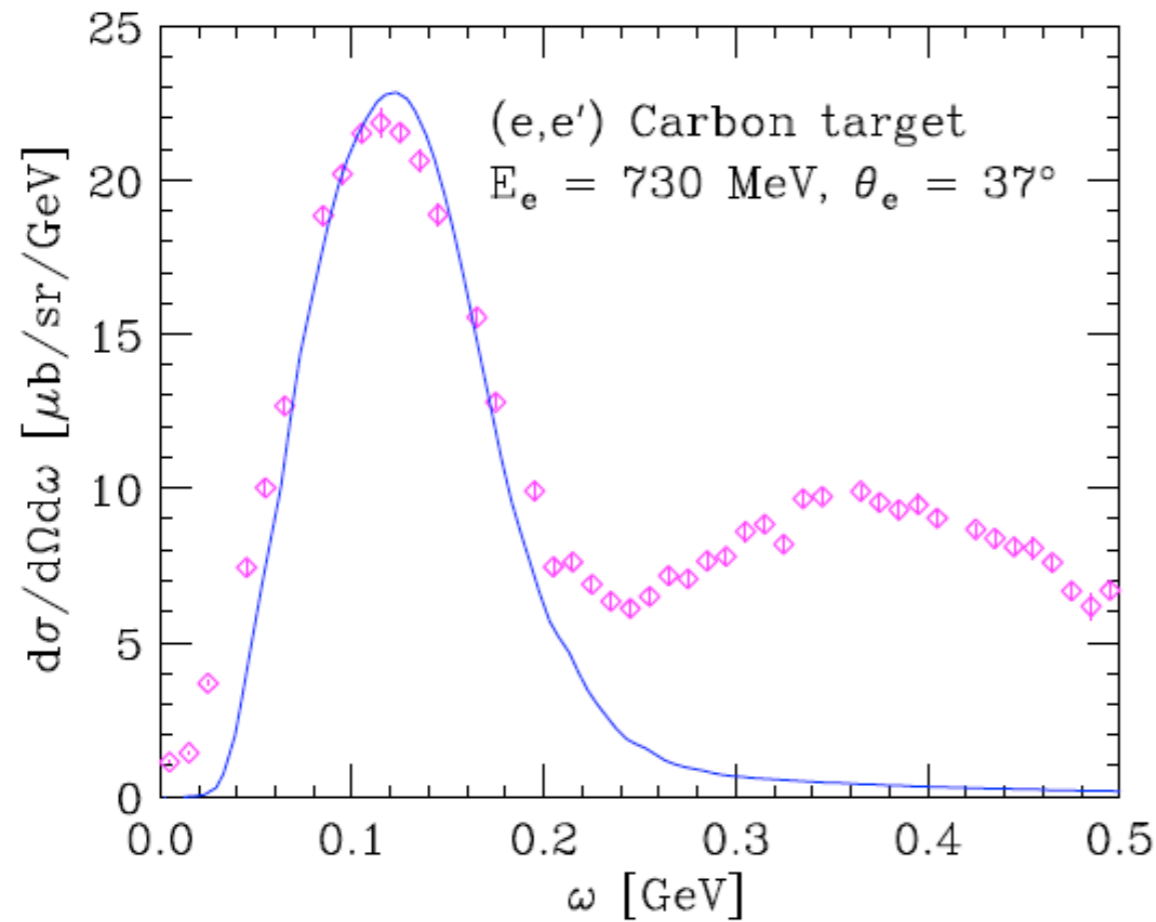
$$\frac{d^2\sigma_{e\alpha}}{d\Omega_{e'} dE_{e'}} = \frac{\alpha^2}{Q^4} \frac{E_{e'}}{E_e} L_{\mu\nu} \mathcal{W}_\alpha^{\mu\nu}.$$

the resulting structure functions, can be written in terms of the vector form factors, F_1 and F_2 , and the axial form factor, F_A

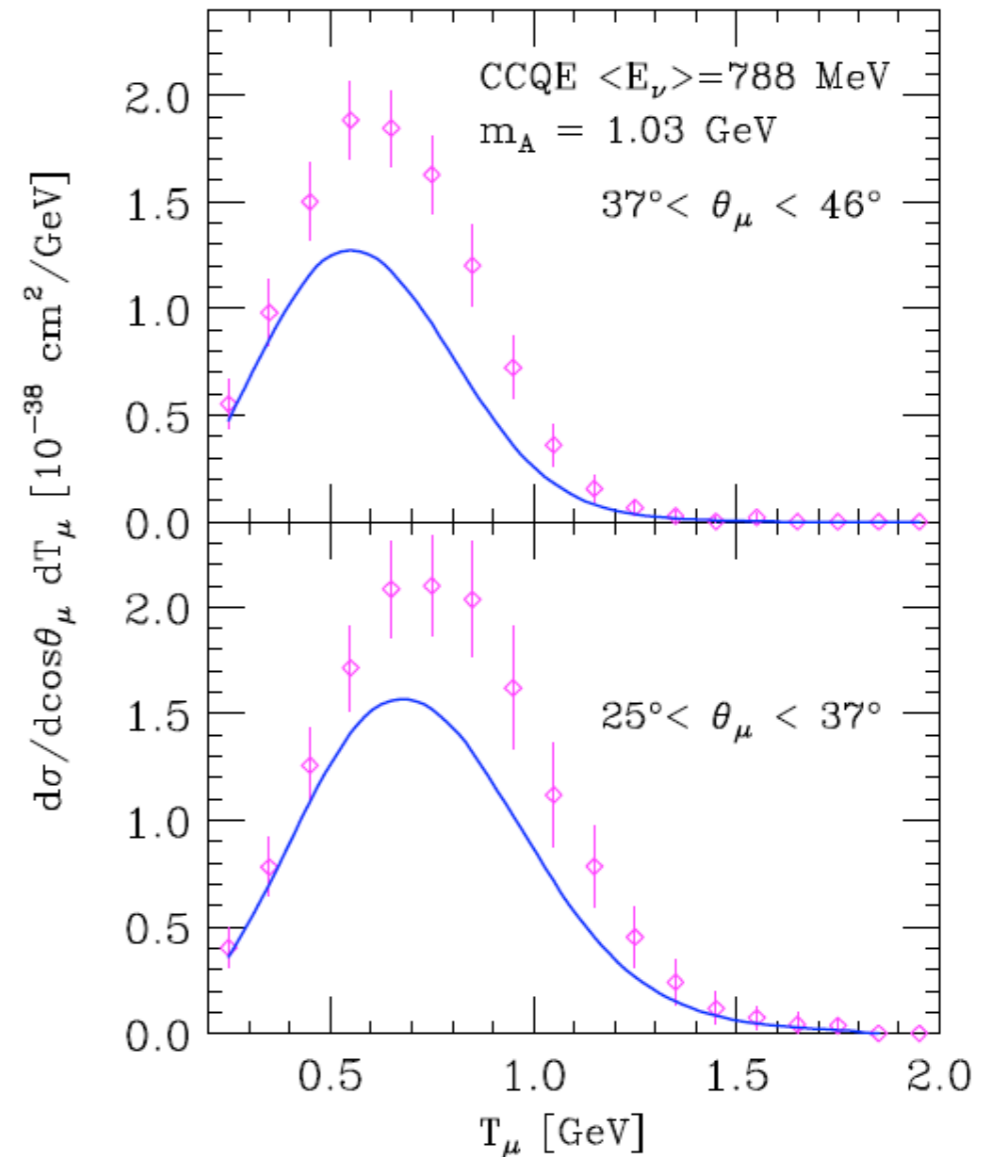
$$F_A(q^2) = g_A \left(1 - \frac{q^2}{m_A^2}\right)^{-2}. \quad (60) \quad m_A = \text{“axial mass”}$$

The axial coupling constant, $g_A = -1.2761_{-17}^{+14}$, is obtained from neutron β -decay (Mund *et al.*, 2013), while the axial mass determined from elastic neutrino- and antineutrino-nucleon scattering, charged pion electroproduction off nucleons and muon capture on the proton is $m_A = 1.03$ GeV (Bernard *et al.*, 2002; Budd *et al.*, 2003).

An effective “quasi-elastic” treatment with 1 nucleon interaction, merely adding the axial current for neutrinos, **not enough**



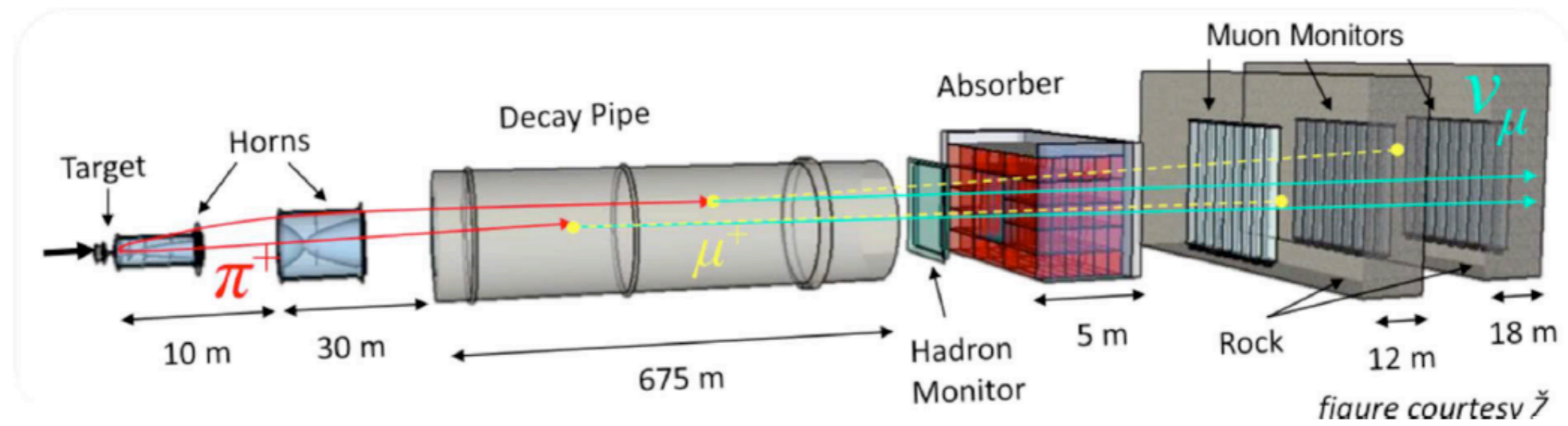
eN



νN

The main difficulty associated with the extension of the theoretical approaches developed for electron-nucleus scattering to the case of neutrino scattering arises from the fact that, since neutrino beams are always produced as secondary decay products, their energy is not sharply defined, but broadly distributed according to a flux Φ .

NuMI Beam line (~same for MINOS, NOvA)



NuMI is a “conventional” neutrino beam, neutrinos from focused pions.

For MINERvA, flux must be calculated, use hadron production data.

Protons on target (POT) to M
 --neutrino (LE): 3.9E20 POT.
 --anti-neutrino (LE): 1.0E20 POT.

Example

In the (anti-)neutrino case, we don't know (precisely and event by event) the initial energy \Rightarrow we do not know q^2

Theory

The main difficulty associated with the extension of the theoretical approaches developed for electron-nucleus scattering to the case of neutrino scattering arises from the fact that, since neutrino beams are always produced as secondary decay products, their energy is not sharply defined, but broadly distributed according to a flux Φ .

The flux-integrated double differential neutrino-nucleus cross section, defined as

$$\frac{d\sigma}{dT_\ell d\cos\theta_\ell} = \frac{1}{N_\Phi} \int dE_\nu \Phi(E_\nu) \frac{d\sigma}{dE_\nu dT_\mu d\cos\theta_\mu}, \quad (52)$$

where $T_\ell = E_\ell - m_\ell$ is the kinetic energy of the outgoing charged lepton and

$$N_\Phi = \int dE_\nu \Phi(E_\nu), \quad (53)$$

1st problem: E_ν has spectrum, not single value

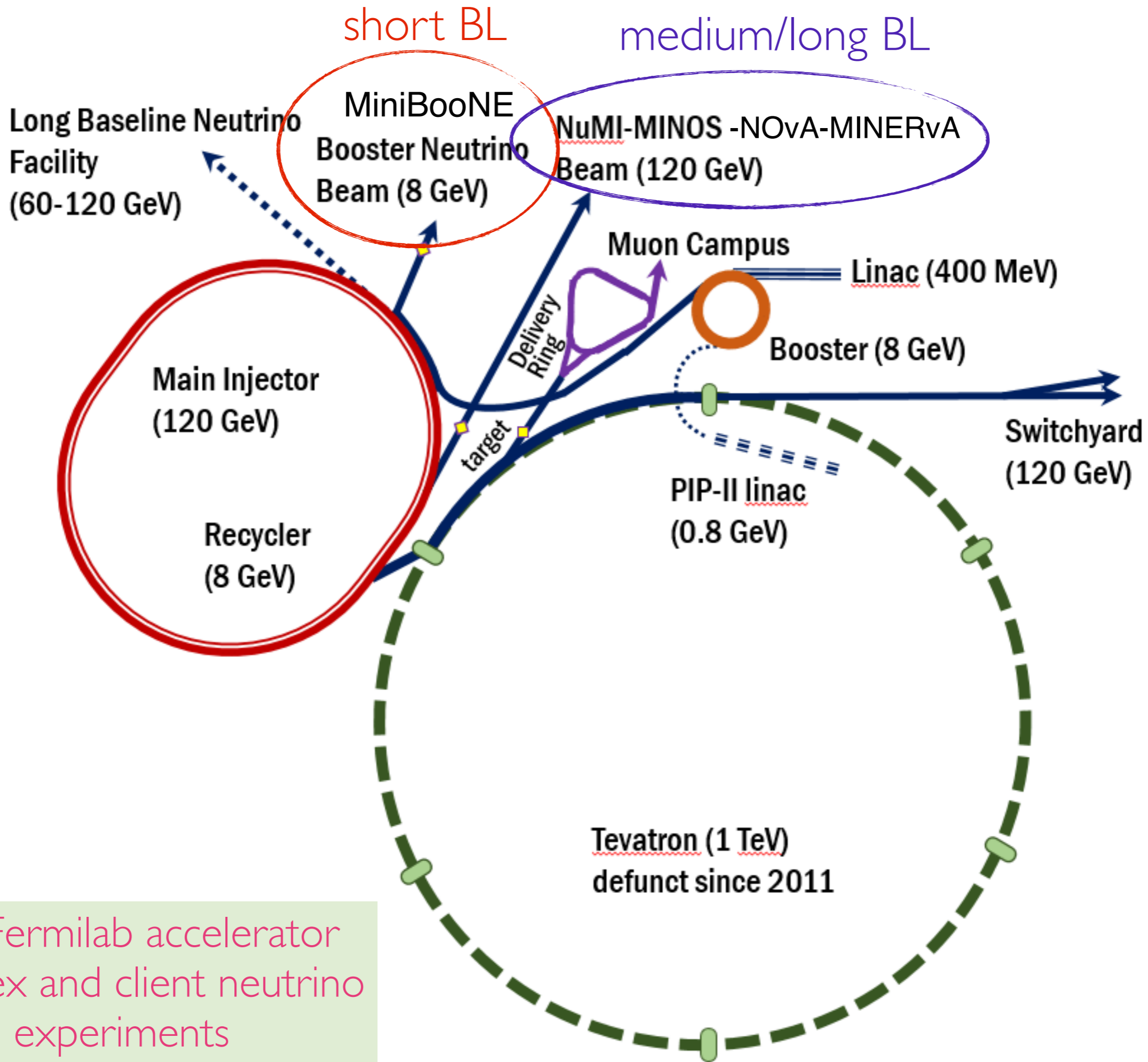
Measurements

Differential Cross section

$$\left(\frac{d\sigma}{dX}\right)_i = \frac{1}{T\Phi} \frac{1}{\Delta X_i} \frac{\sum_j U_{ij} (N_j^{data} - N_j^{bkg})}{\epsilon_i}$$

Total Cross section

$$\sigma(E_\nu)_i = \frac{1}{T\Phi_i} \frac{\sum_j U_{ij} (N_j^{data} - N_j^{bkg})}{\epsilon_i}$$



The Fermilab accelerator complex and client neutrino experiments

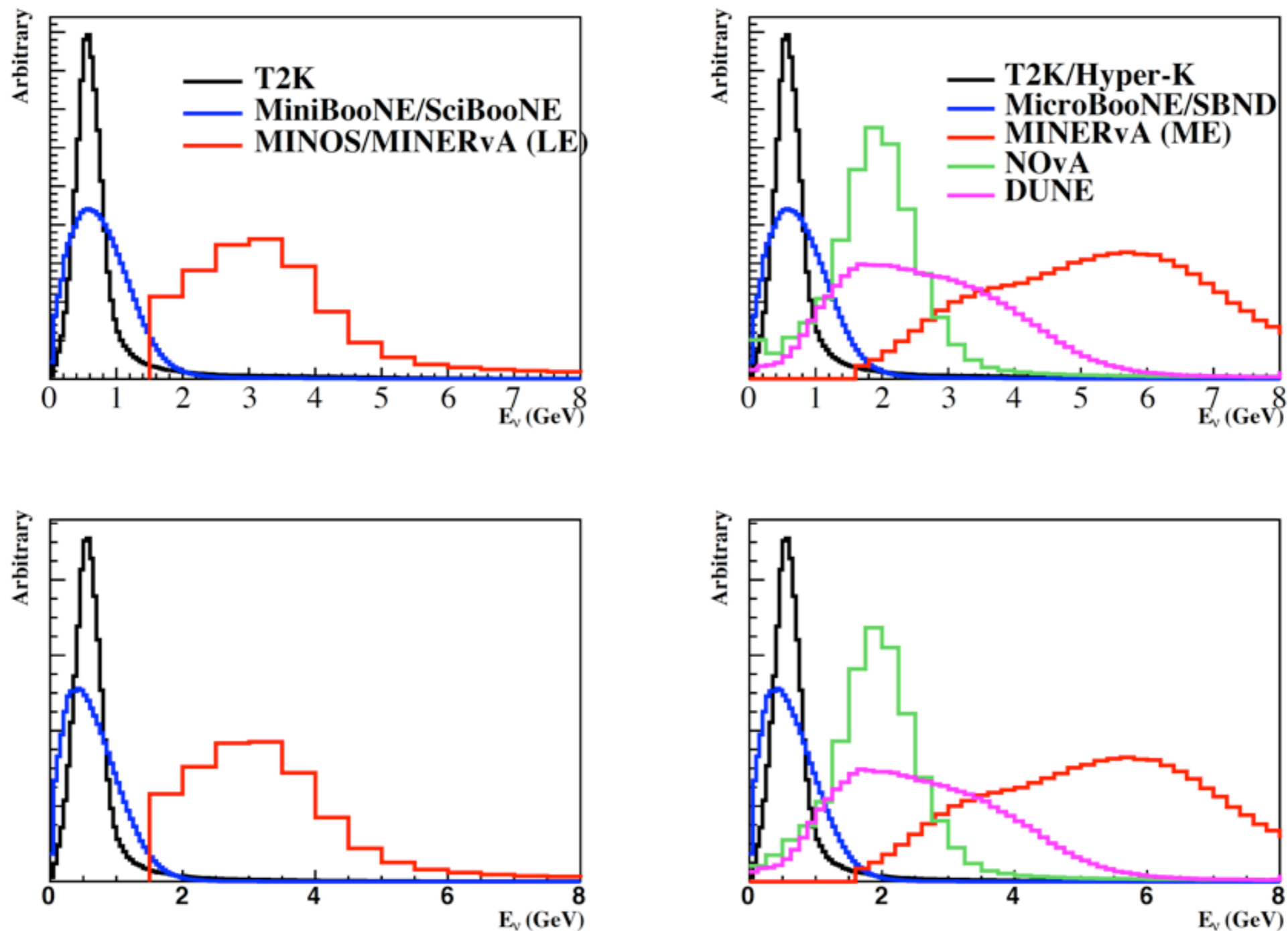


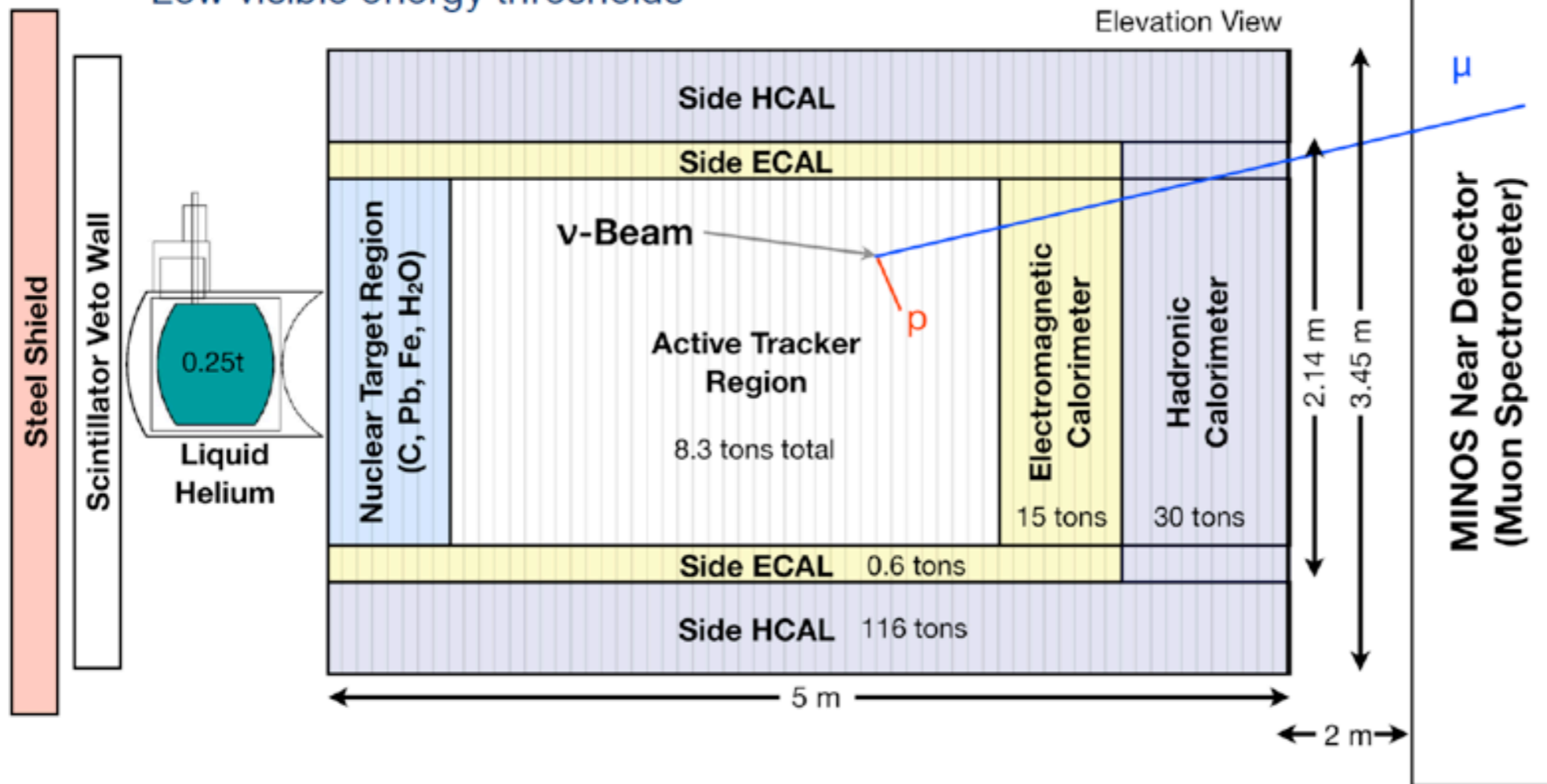
Figure 3. Muon neutrino and muon anti-neutrino flux predictions from current and future accelerator based neutrino experiments. Here, the top two plots are neutrino mode beam muon neutrino flux predictions, where the bottom two plots are anti-neutrino mode beam muon anti-neutrino flux predictions. Predictions are all arbitrary normalized. Left plots are current experiments (T2K, MiniBooNE, MINERvA with low energy NuMI), and right plots are current to future experiments (Hyper-Kamiokande, MicroBooNE, NOvA, DUNE, MINERvA with medium energy NuMI).

MINERvA Detector



Solid Scintillator (CH) Tracker

- Tracking, particle ID, calorimetric energy measurements
- Low visible energy thresholds



MINOS Near Detector

- Provides muon charge and momentum

Nuclear Targets

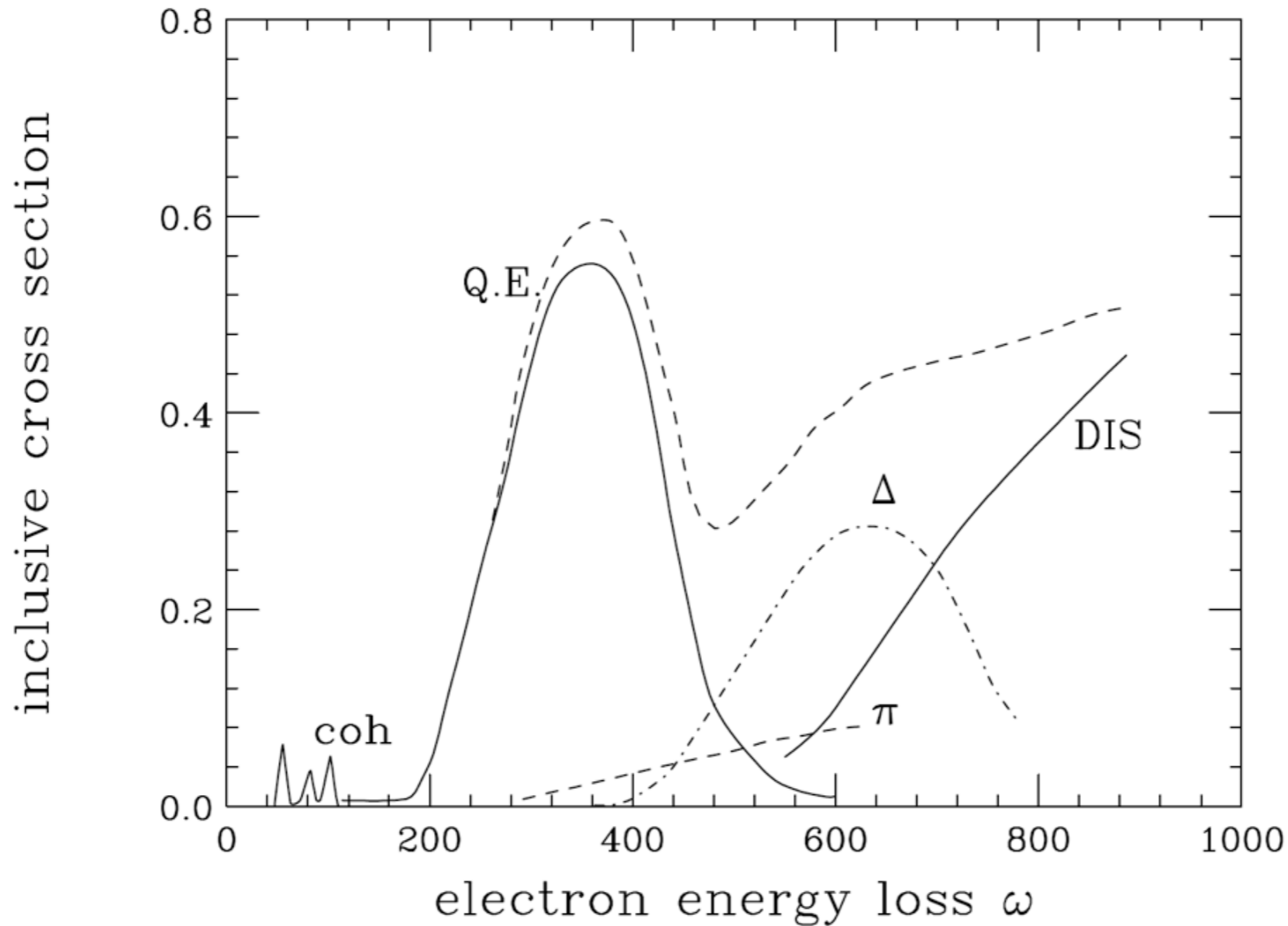
- Allows side by side comparisons between different nuclei
- Pure C, Fe, Pb, LHe, water

Side and Downstream Electromagnetic and Hadronic Calorimeters

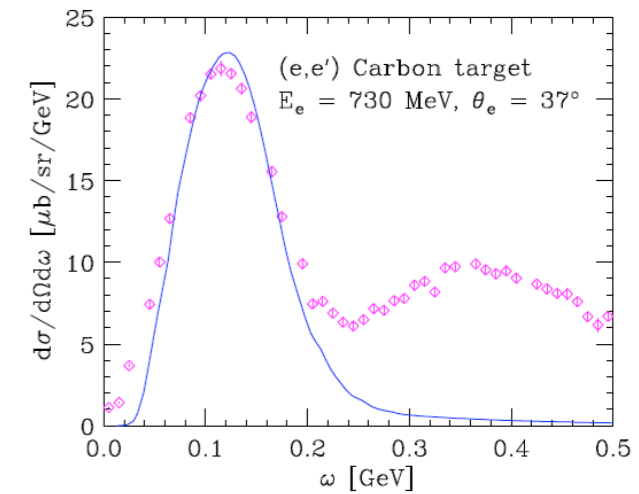
- Allow for event energy containment



Two fold problem, connected with sampling different q^2 in a non-monochromatic flux



**2nd problem:
not just QE**



$$\omega = T_e^{\text{ini}} - T_e^{\text{fin}}$$

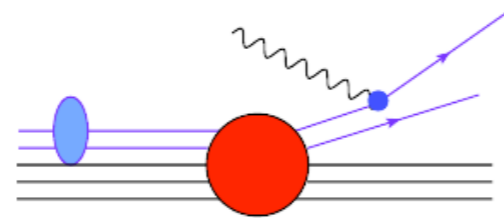
FIG. 1 Schematic representation of the inclusive electron-nucleus cross section at beam energy around 1 GeV, as a function of the energy transfer (Benhar *et al.*, 2008).

The **TWO** concurring effects:

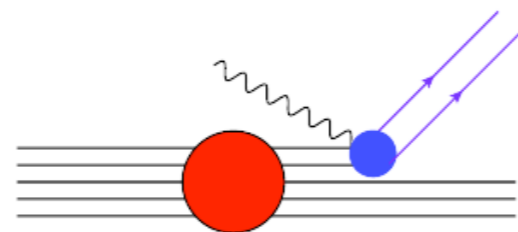
1. In the (anti-)neutrino case we do not know q^2 - we sample different “ ω ” values
 - changing relative importance of DIS, RES wrt CCQE
2. Additional N-N interactions \Rightarrow the Impulse Approximation, with no other interactions than the recoil of the involved nucleon, is not enough
 - remember: “CCQE” = events with “0 pions”

In a model accounting for NN correlations, 2p2h final states can be produced through 3 different reaction mechanisms.

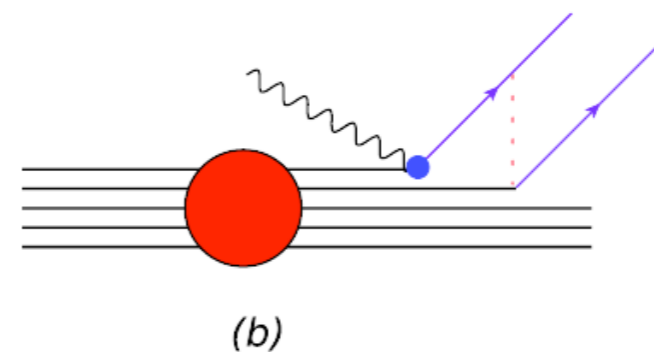
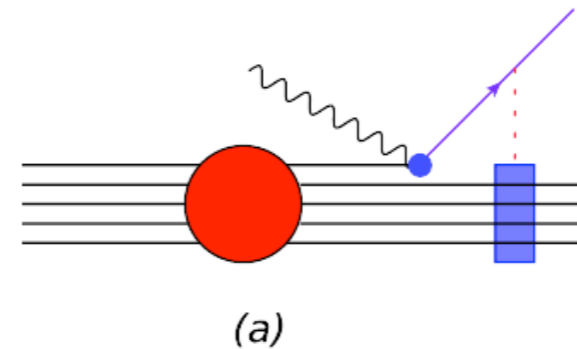
- Initial State Correlations (ISC):



- Meson Exchange Currents (MEC):

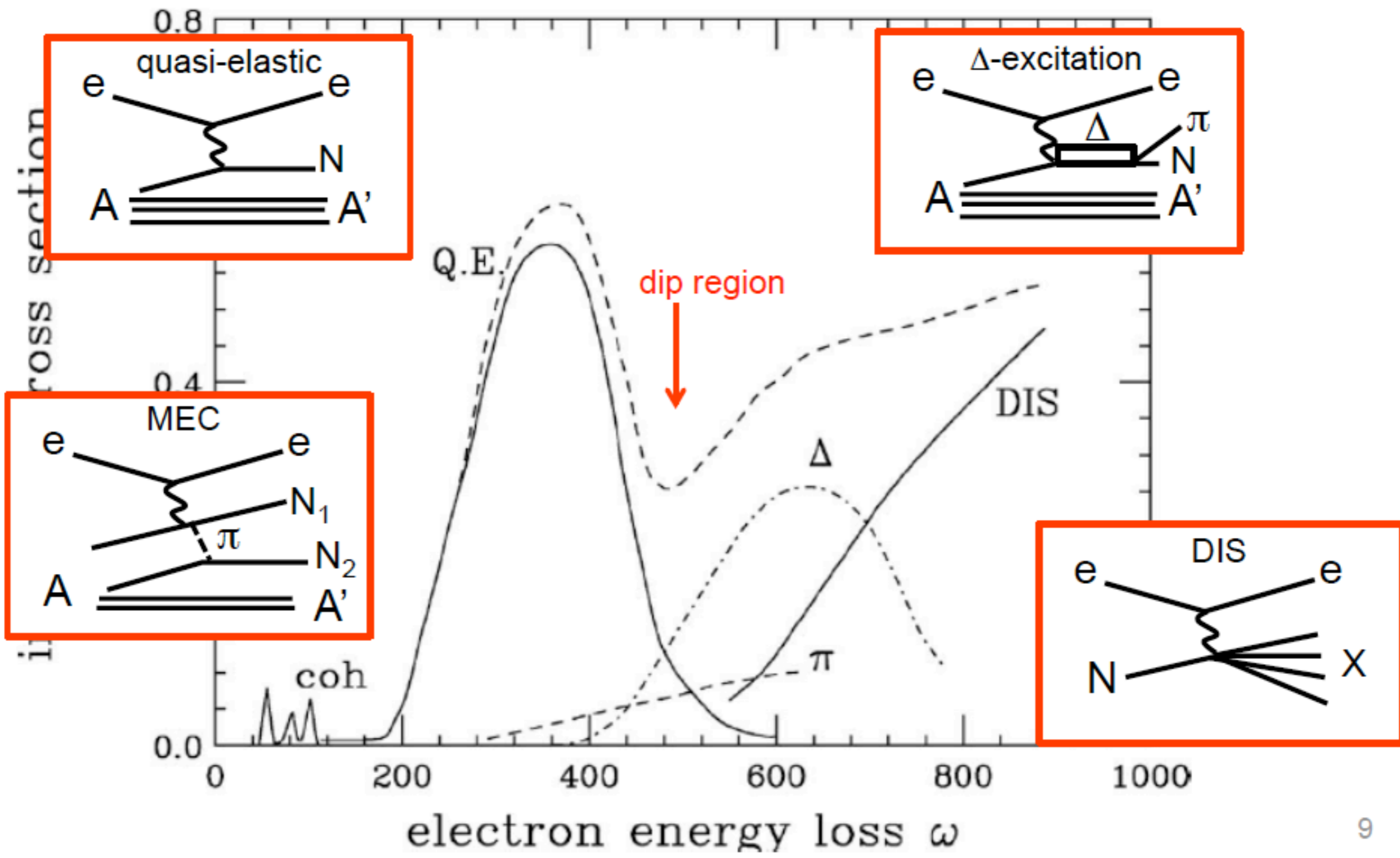


- Final State Interactions (FSI):



“2 particles-2 holes”, see later

Inclusive electron scattering with function of energy loss



0/22/12

9

Correlated nucleon interactions

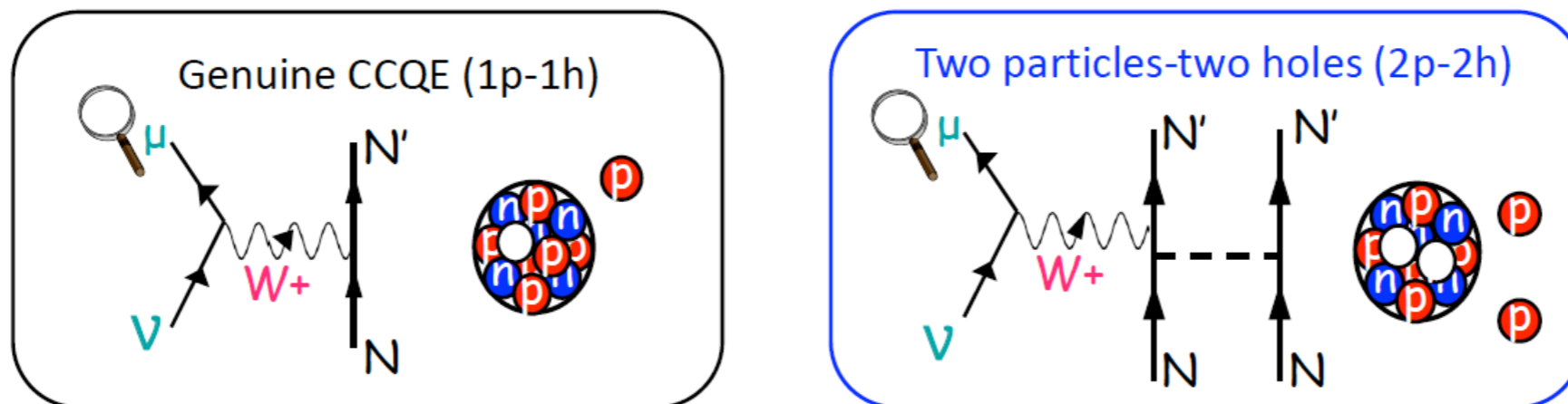


Figure 14. Schematic and pictorial representation of the 1p-1h and 2p-2h excitations.

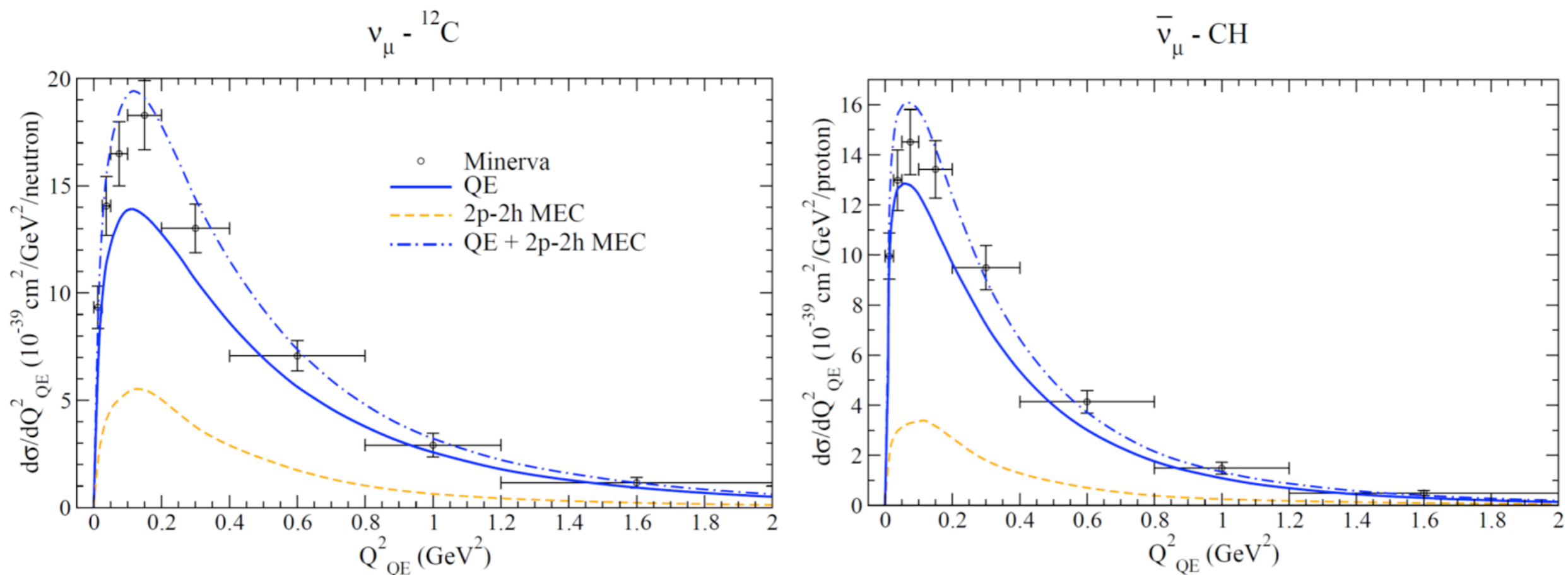
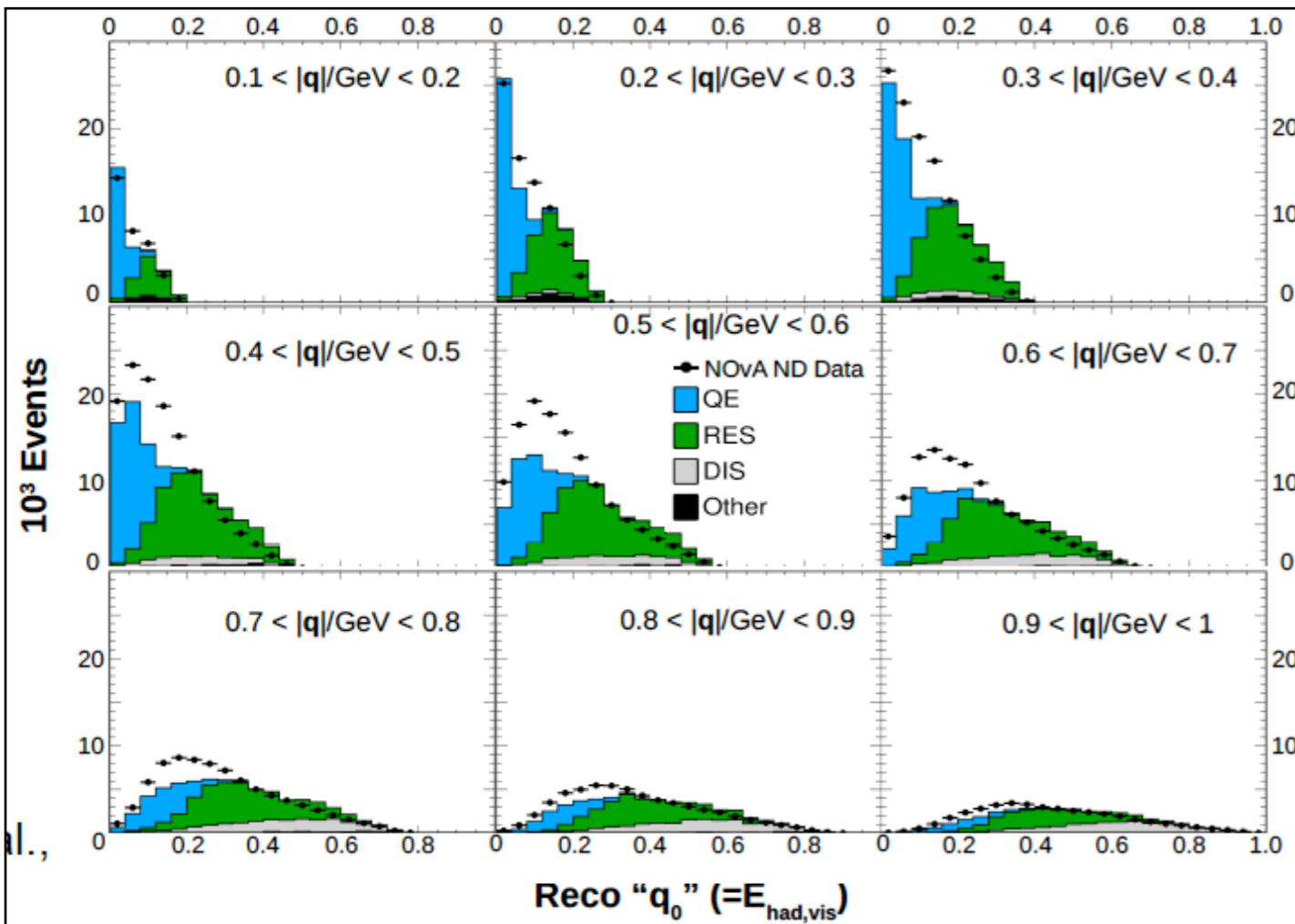
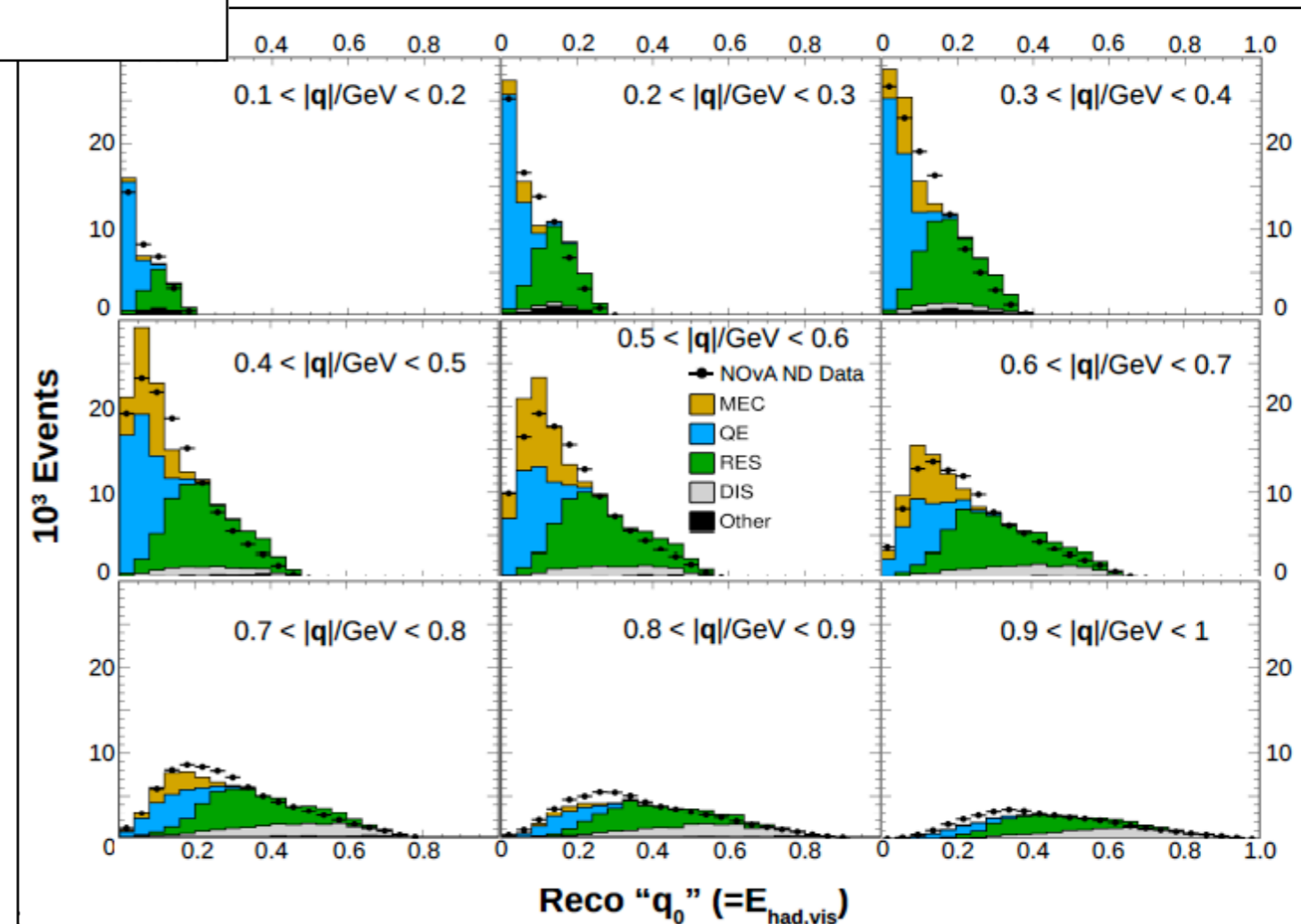
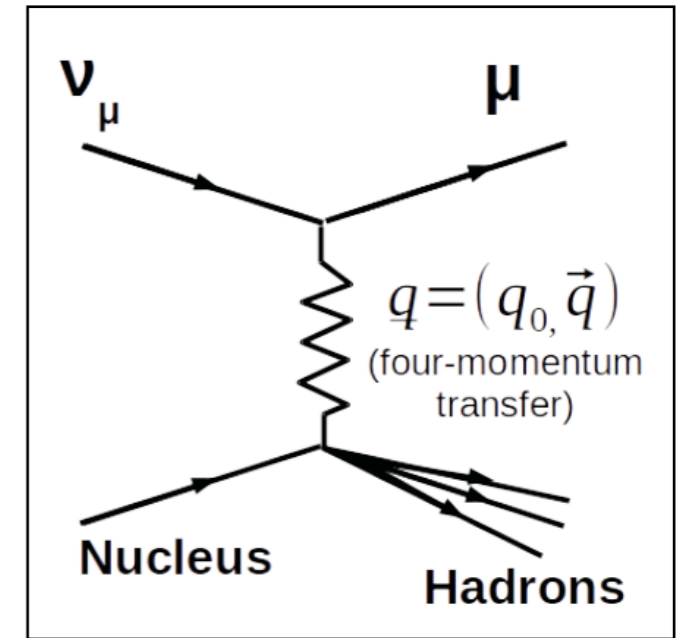


Figure 25. The MINERvA flux-integrated Q^2 distributions calculated by Megias *et al.* [209] compared with the new preliminary MINERvA neutrino and antineutrino CCQE-like data.

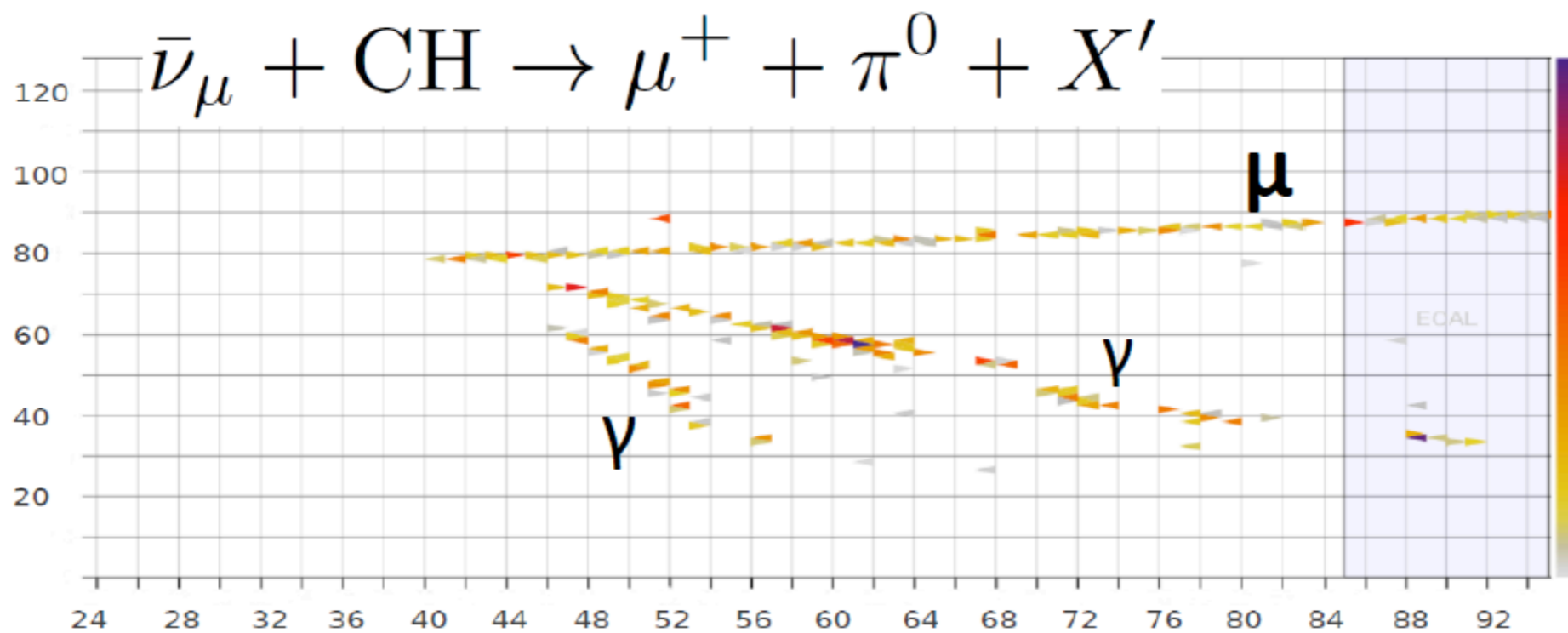
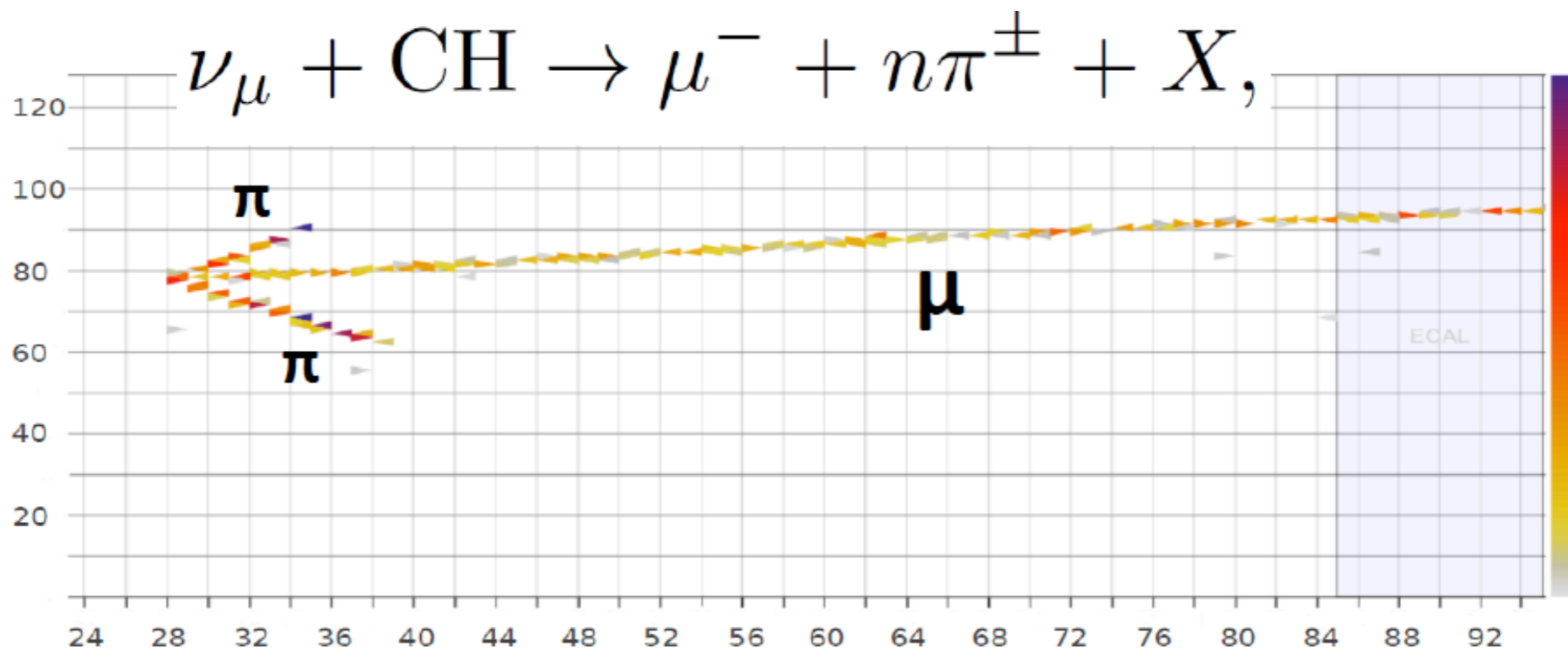


baseline GENIE MC



- Enable GENIE empirical Meson Exchange Current Model
- Reweight to match NOvA excess as a function of 3-momentum transfer

Signatures in MINERvA, dedicated measurements of >0 π events



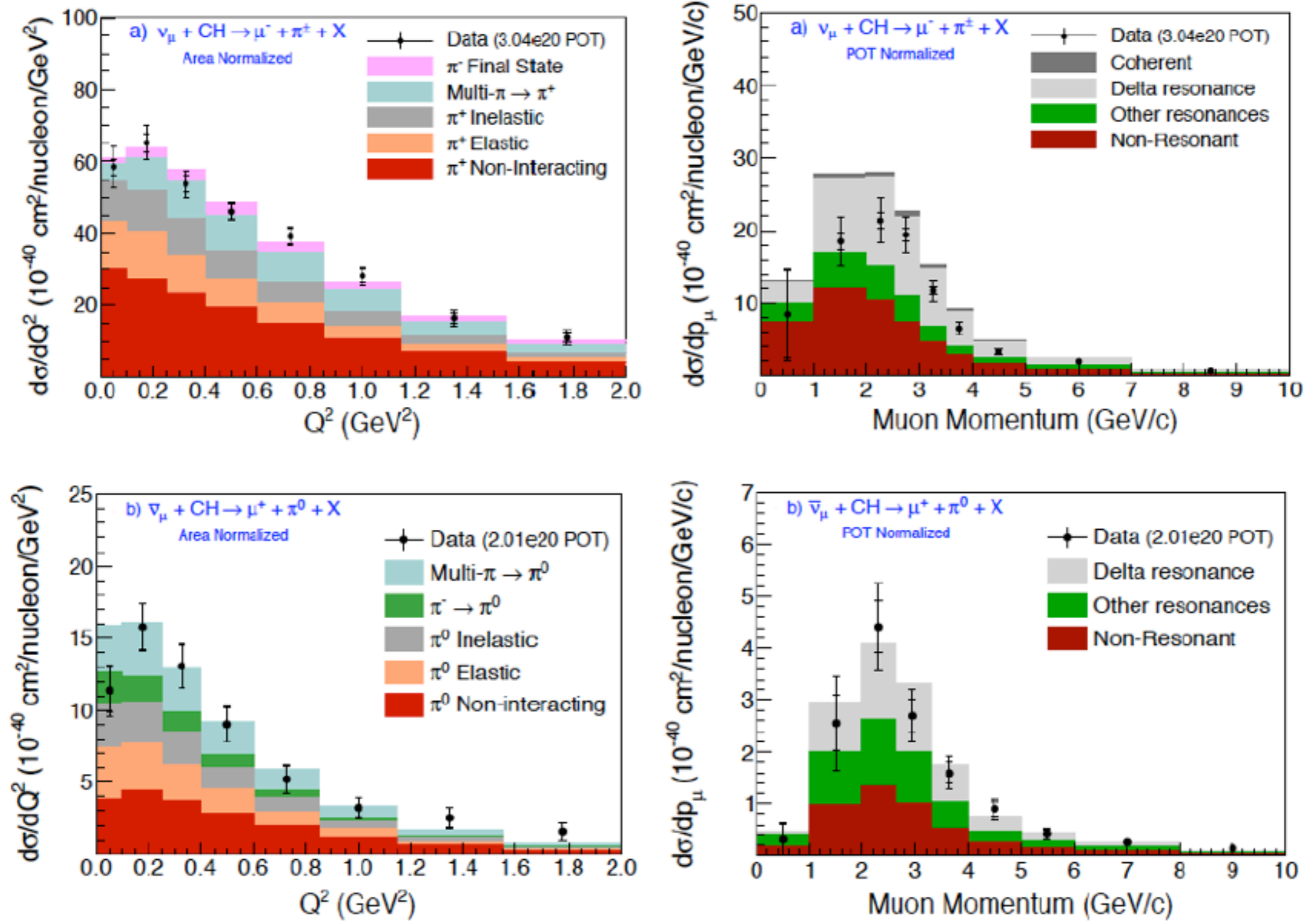
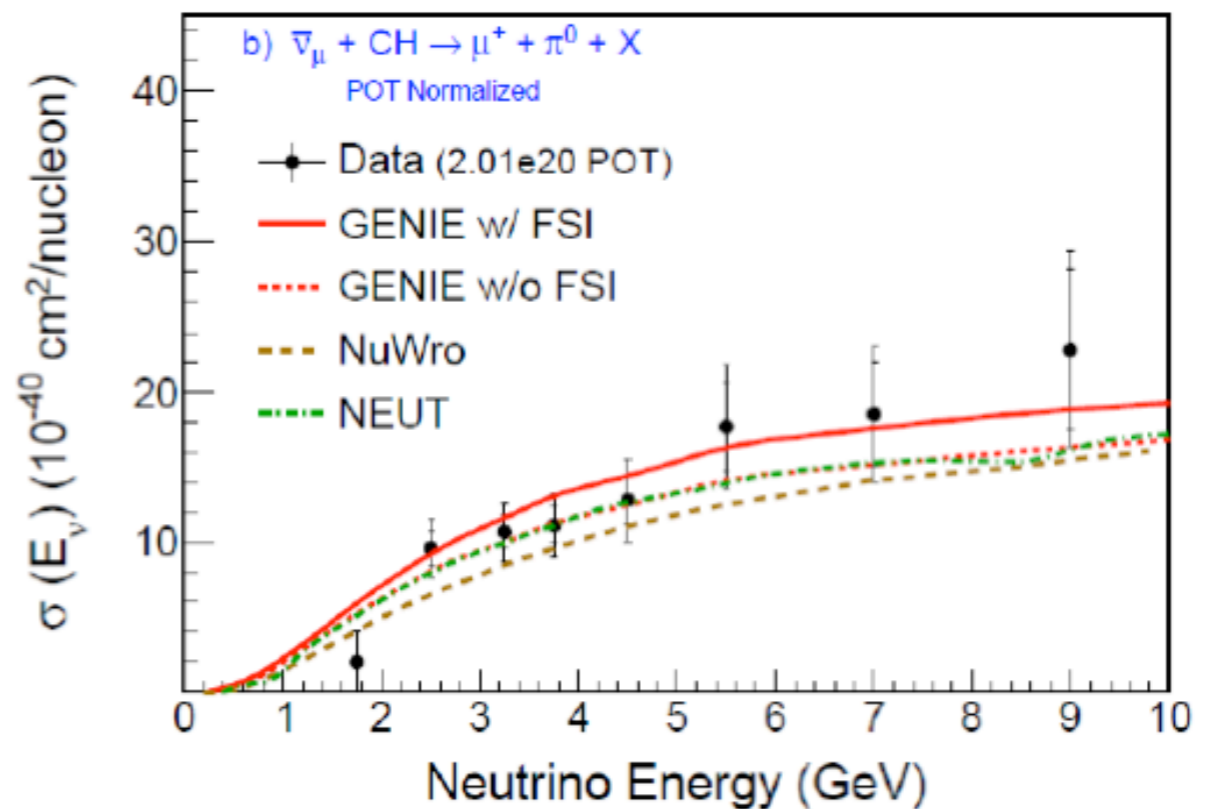
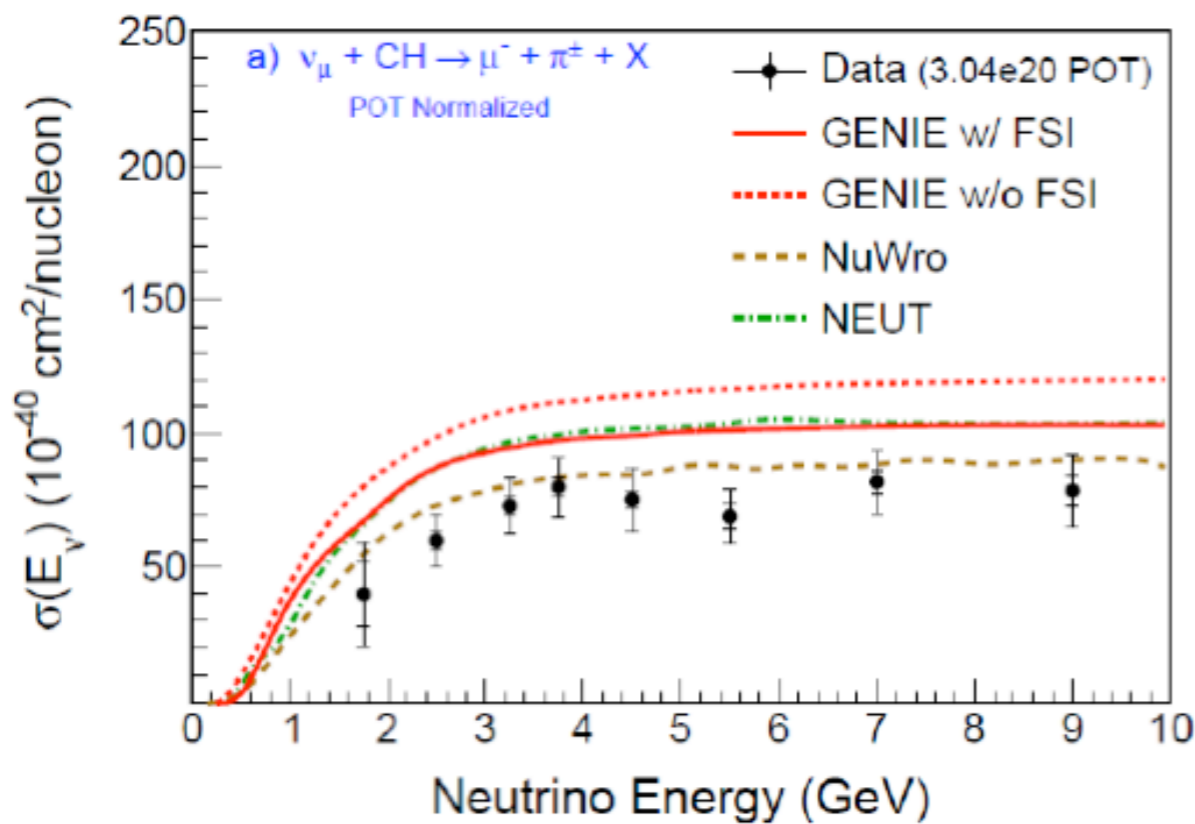
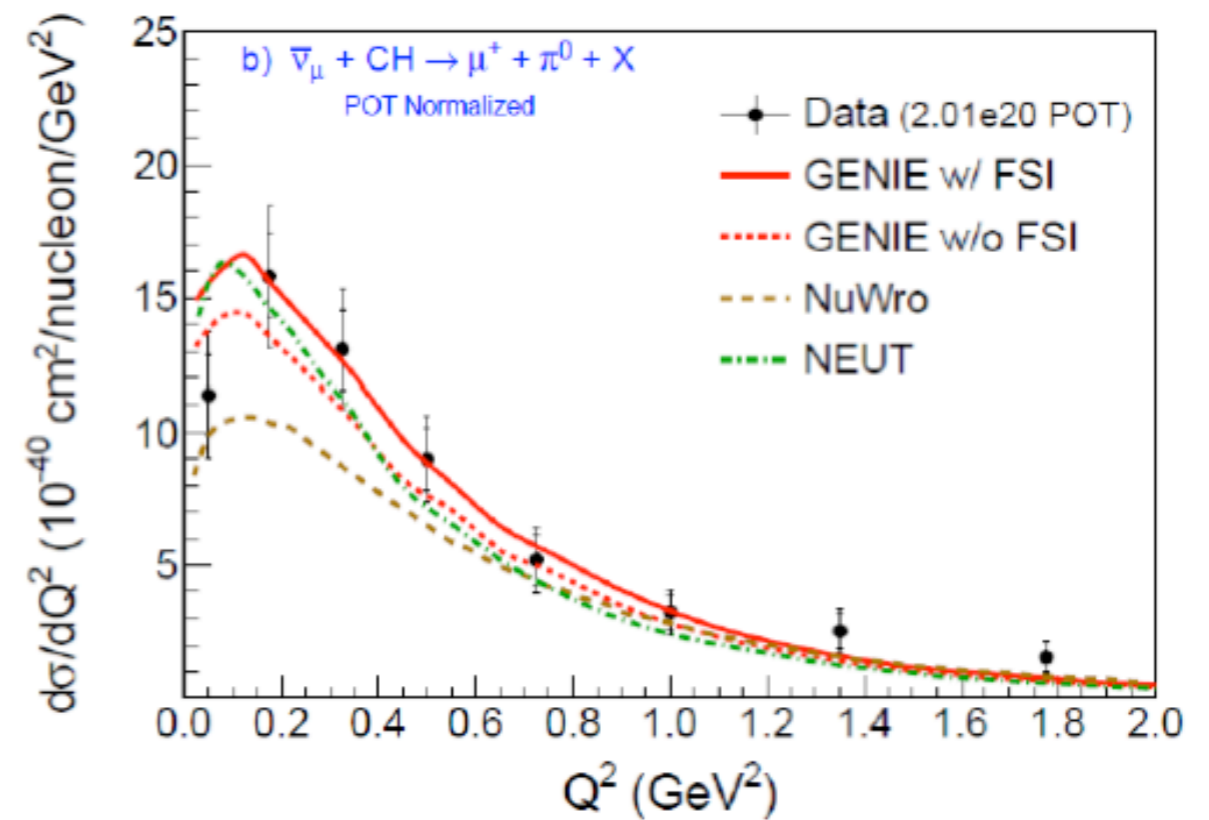
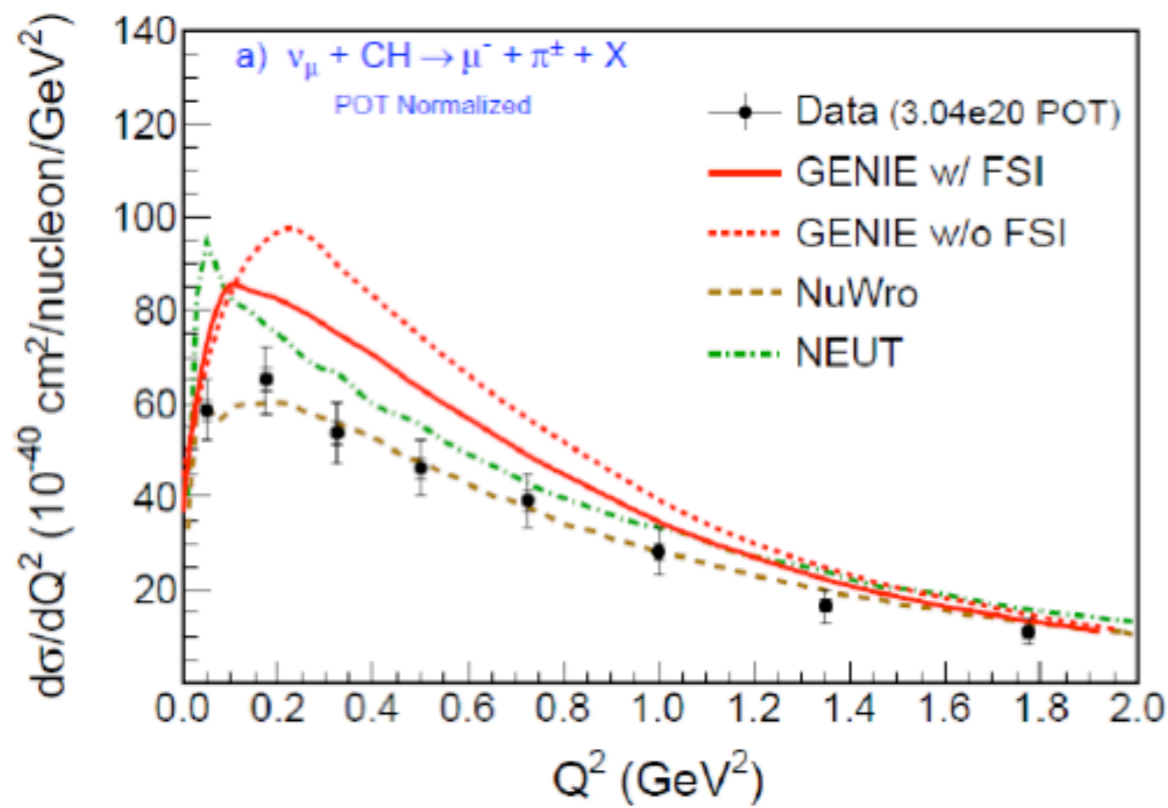


Figure 34. Neutrino $CC1\pi^+$ (top) and antineutrino $CC1\pi^0$ (bottom) production flux-integrated differential cross section, with function of Q^2 (left) and μ momentum (right) [120]. In the left plot, measured cross section is compared with GENIE prediction decomposed with different FSI components. In the right, measured cross section is compared with GENIE prediction decomposed with different primary interactions. Note left plots are area normalized.

MINERvA



These sort of “service” measurements allow to compare and tune the various MC models

Effect on oscillation measurements

What is measured

- $N(\nu_\mu)$ produced from a pion beam, then disappeared
- $N(\nu_e)$ appearing in a ν_μ flux from a pion beam

ν_μ disappearance:

$$P(\nu_\mu \rightarrow \nu_\mu) \approx 1 - \underbrace{\sin^2 2\theta_{23}}_{\text{...to leading order}} \sin^2(\Delta m_{32}^2 L / 4E)$$

experimental data are **consistent with unity**
("maximal mixing")

➔ Need a leap in precision on θ_{23} (and Δm_{32}^2)

ν_e appearance:

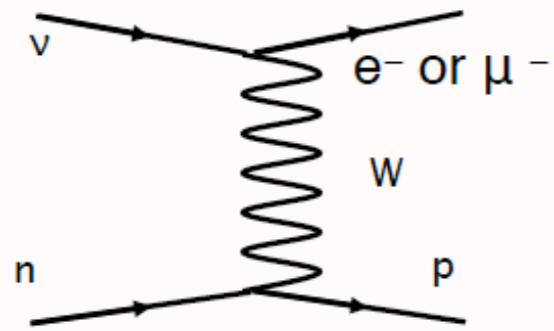
$$P(\nu_\mu \rightarrow \nu_e) \approx \sin^2 \theta_{23} \underbrace{\sin^2 2\theta_{13}}_{\text{...plus potentially large CPv and matter effect modifications!}} \sin^2(\Delta m_{32}^2 L / 4E)$$

Daya Bay reactor experiment:
 $\sin^2(2\theta_{13}) = 0.084 \pm 0.005$

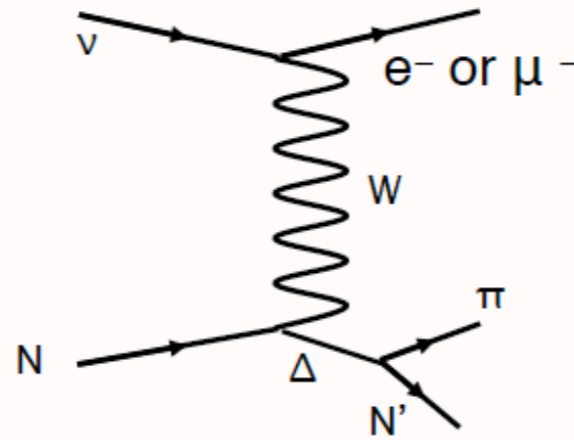
Crucial to know flux:

- $N(\nu_\mu, t=0)$
- E spectrum

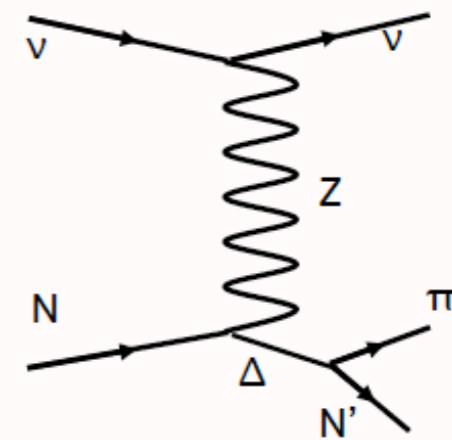
Charged-Current Quasi-Elastic (CCQE)



Charged-Current π

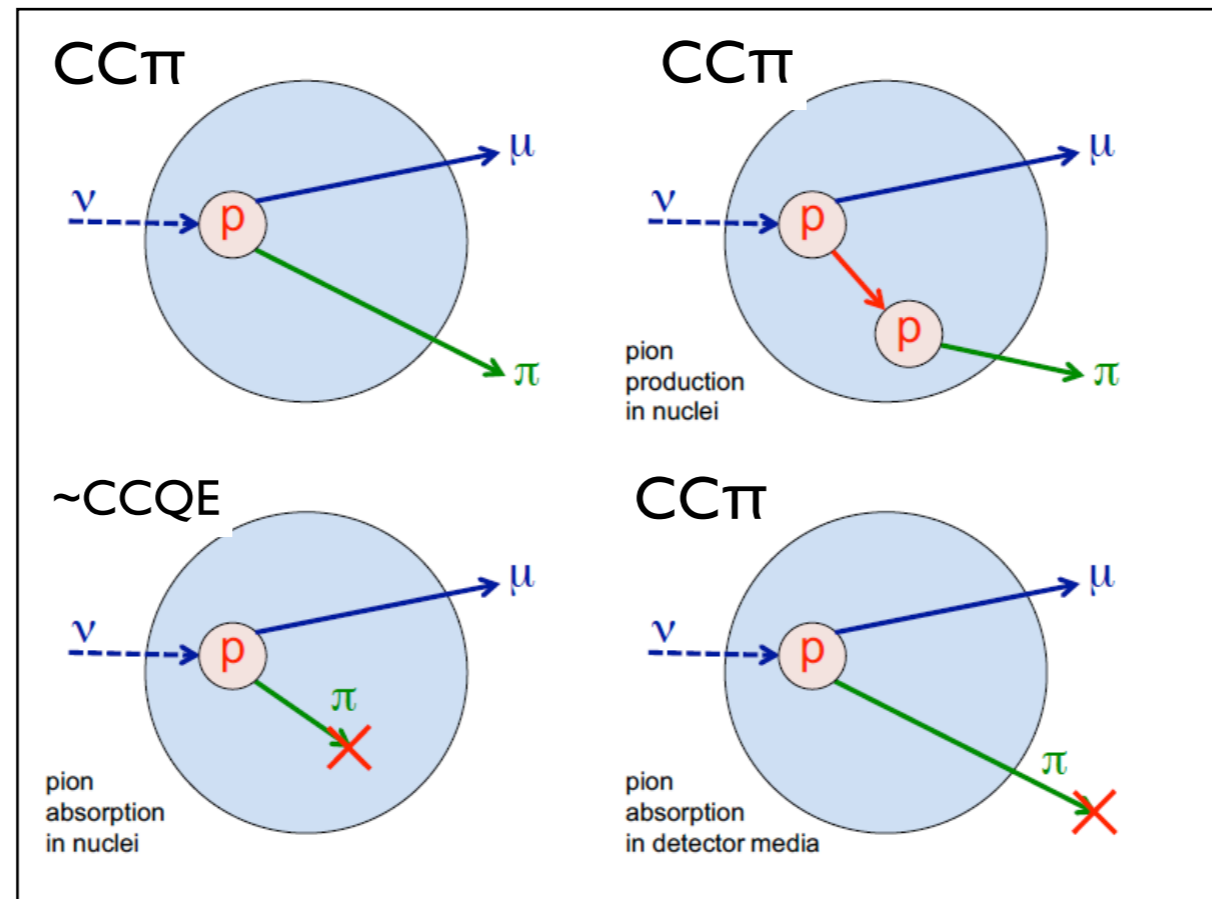


Neutral-Current π

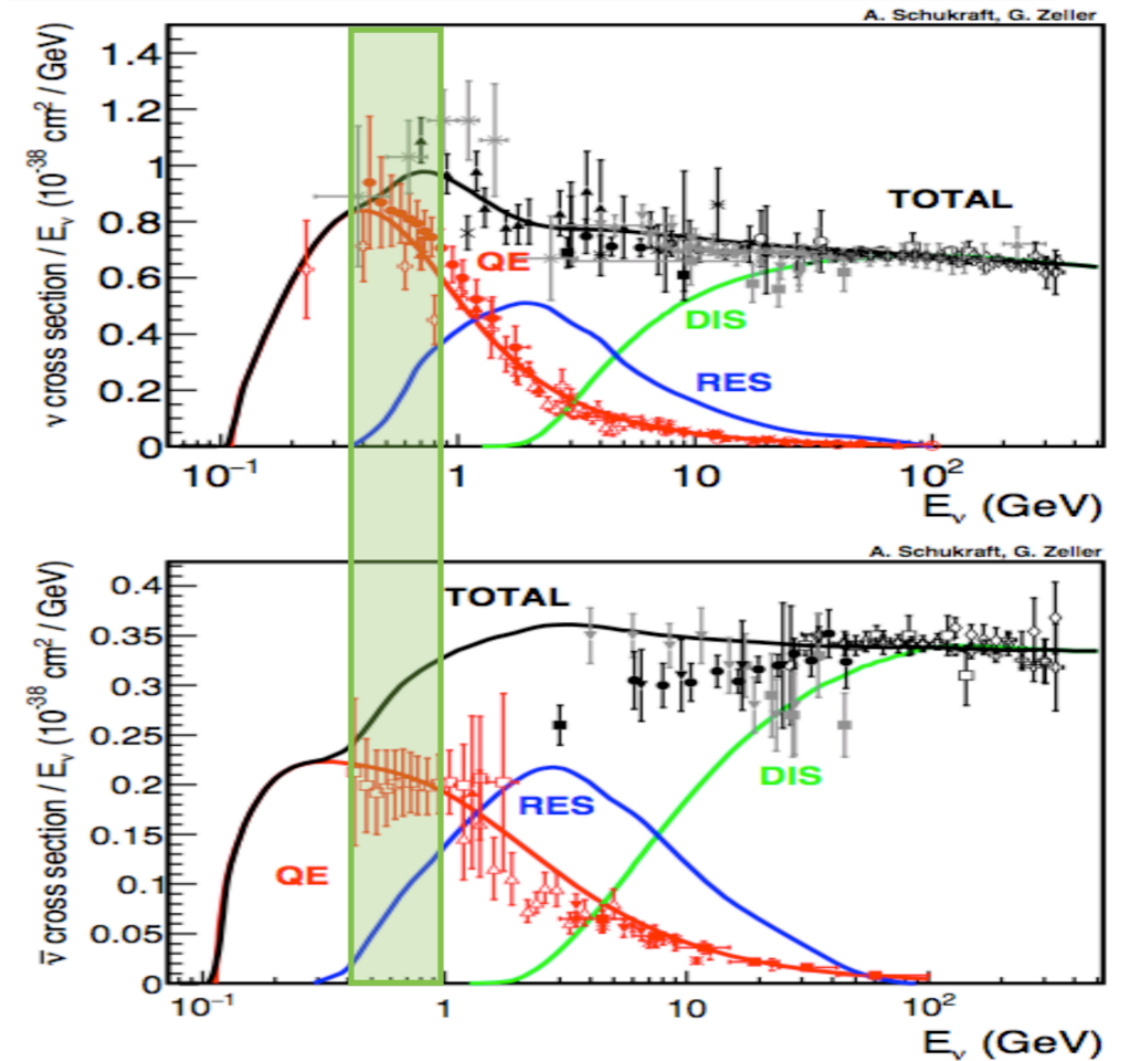
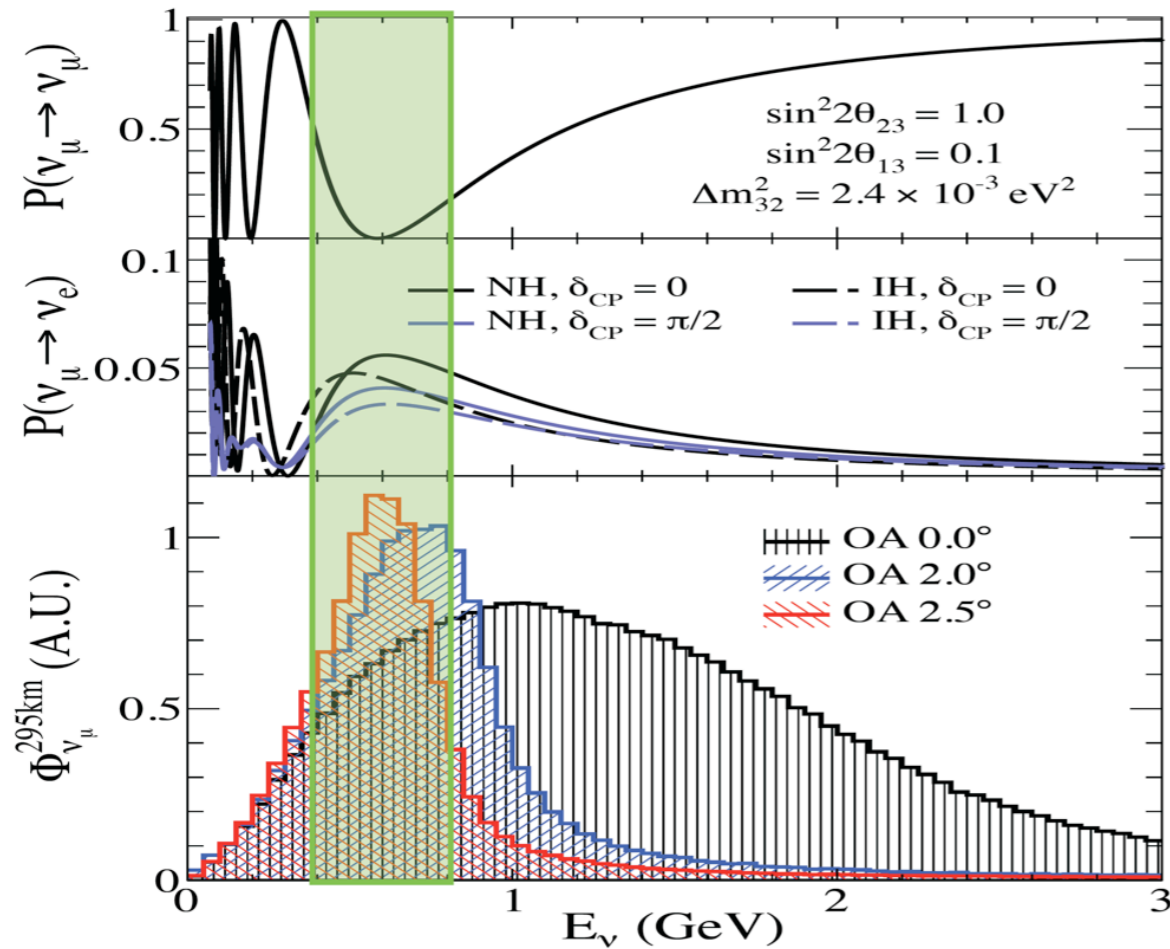
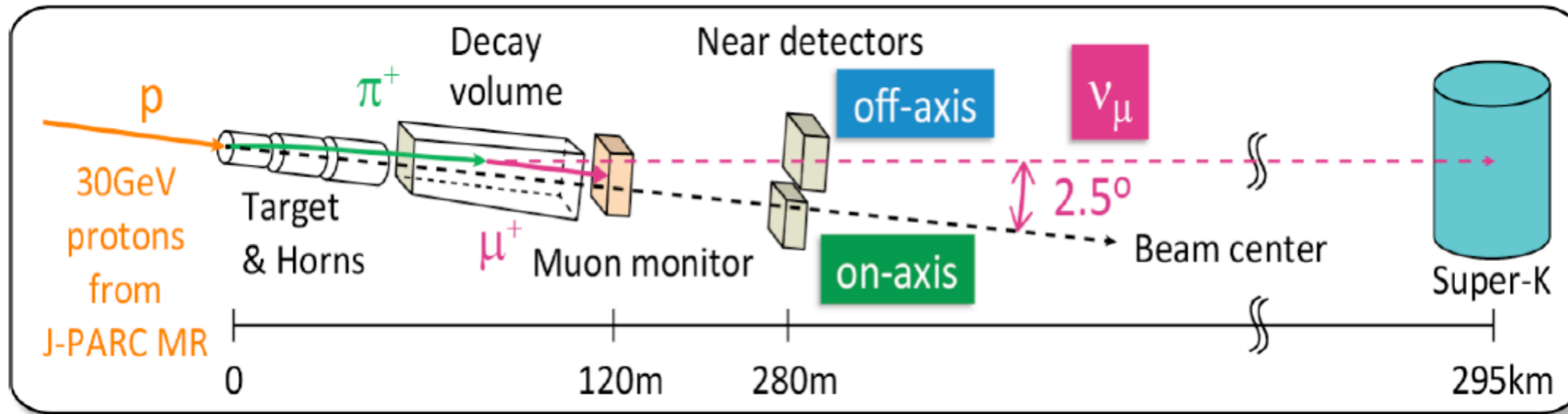


Other cross-section components

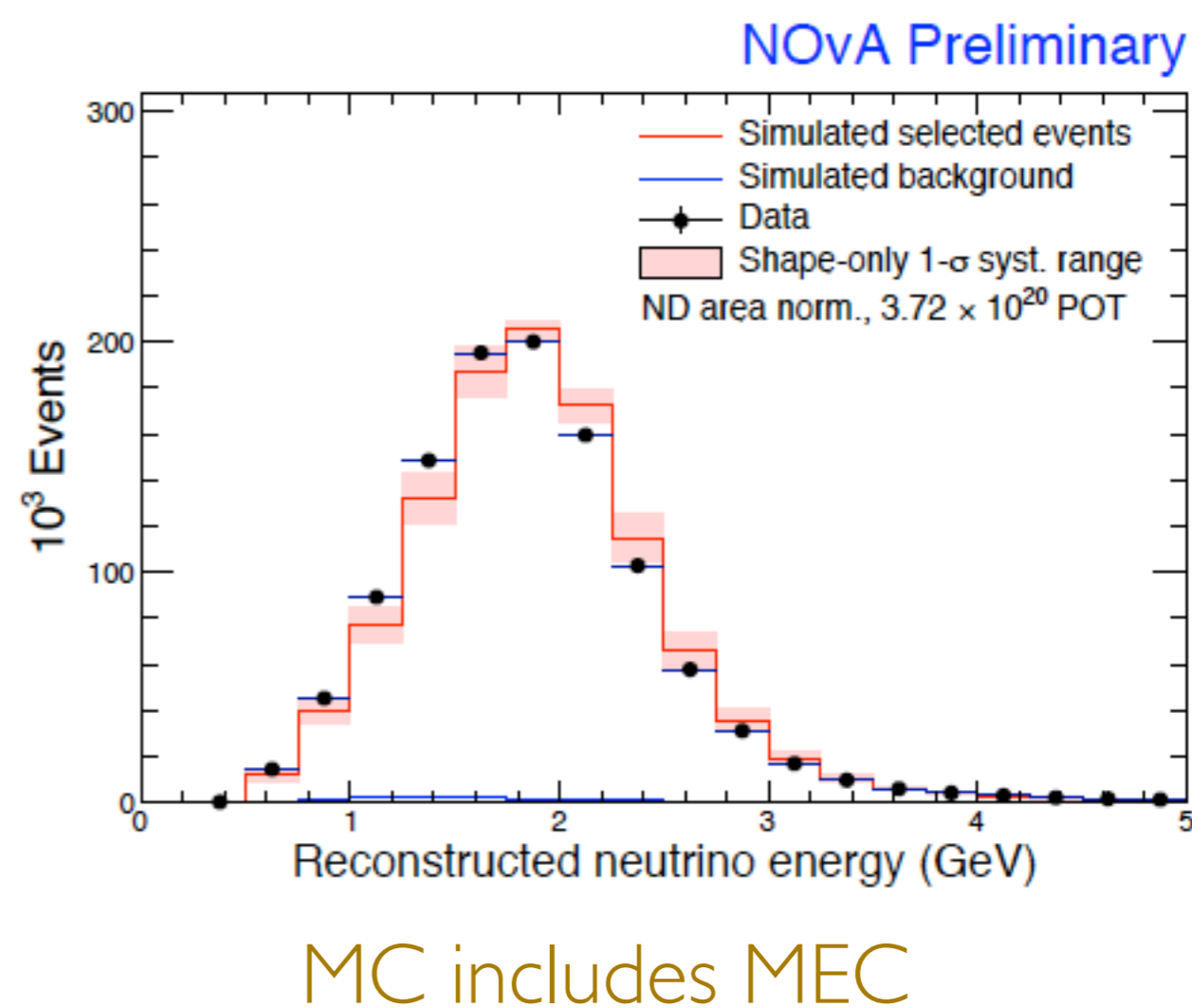
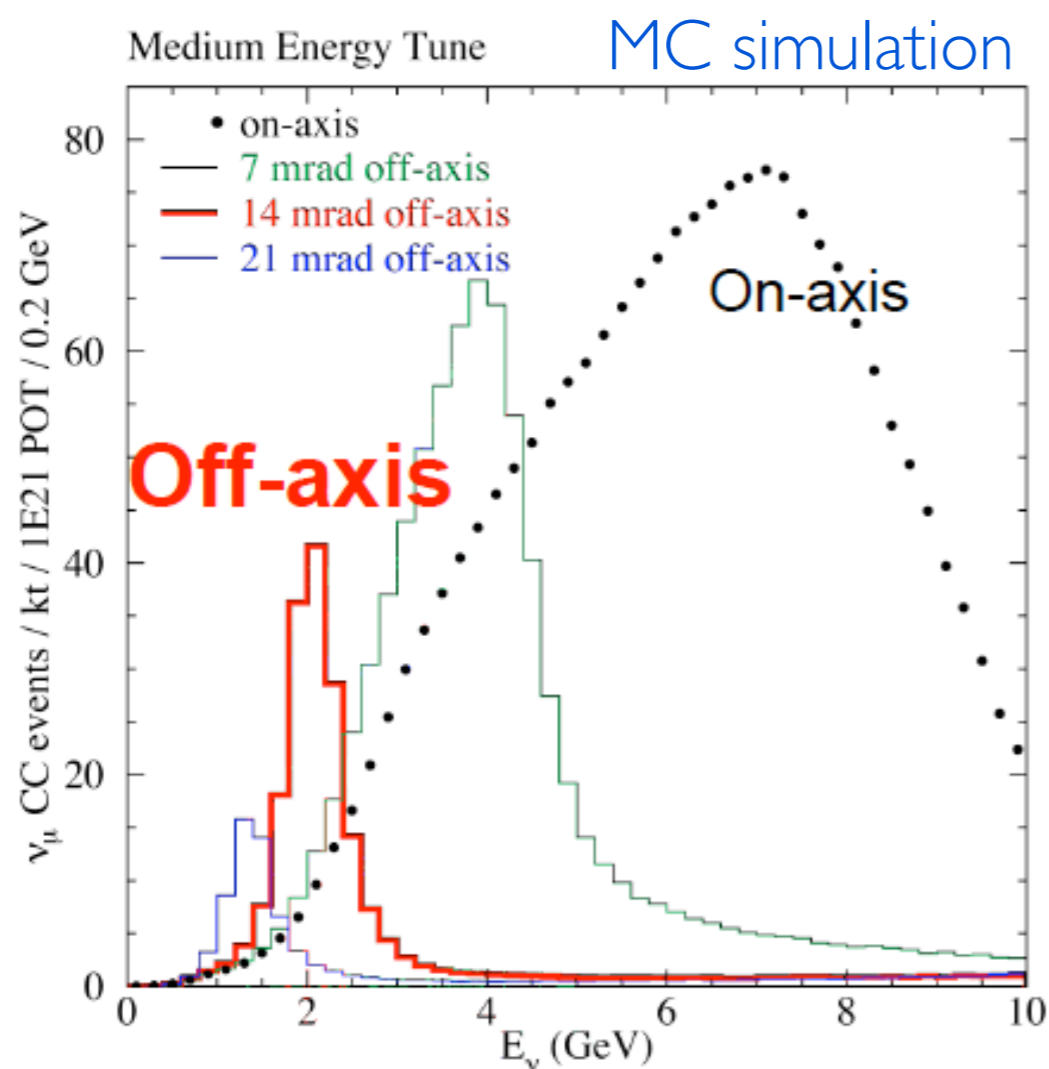
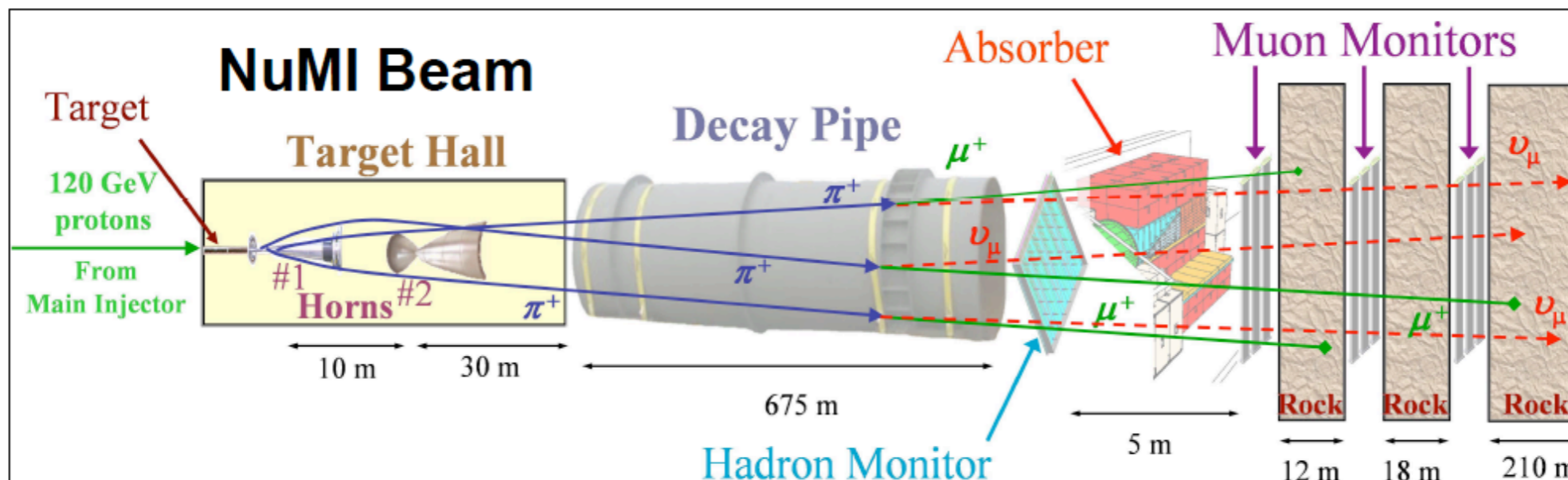
- CCQE-like multinucleon interaction (2 nucleons in the final state)
- Charged-current single-pion production (CCπ)
- Neutral-current single-pion production (NCπ)



Design principle: the off-axis angle

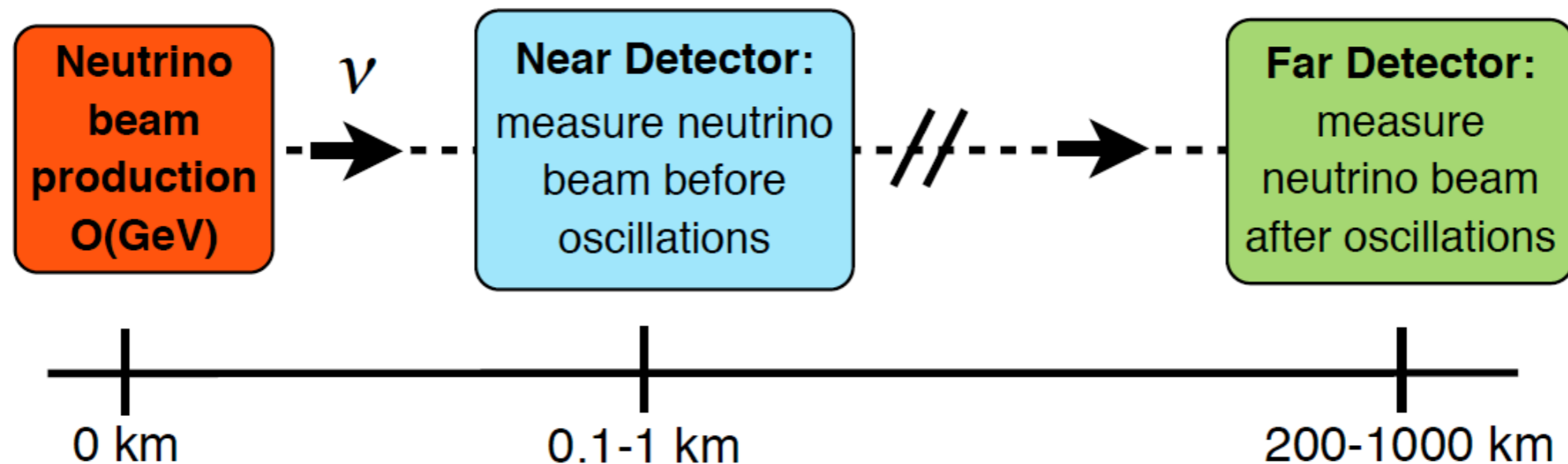


Typical energies from $O(10^2 \text{ MeV})$ to $\sim 1 \text{ GeV}$



Typical energies from $O(10^2 \text{ MeV})$ to $\sim 10 \text{ GeV}$

- Difficult to know neutrino flux at “final” detector
- That also affects absolute rate of ν -N interaction
 - Would like to check ν -N x-sec *in situ*
 - Usually build a Near-Detector similar to the main one (FD)
 - ideally: same type of materials and dimensions = acceptance
 - normalize $N(\text{FD})$ to $N(\text{ND})$ and cancel systematics
 - not entirely possible, residual systematic uncertainties remain tricky to estimate



Near Detector: $N_{ND} \sim \Phi(E_\nu) \sigma(E_\nu) \epsilon_{ND}$

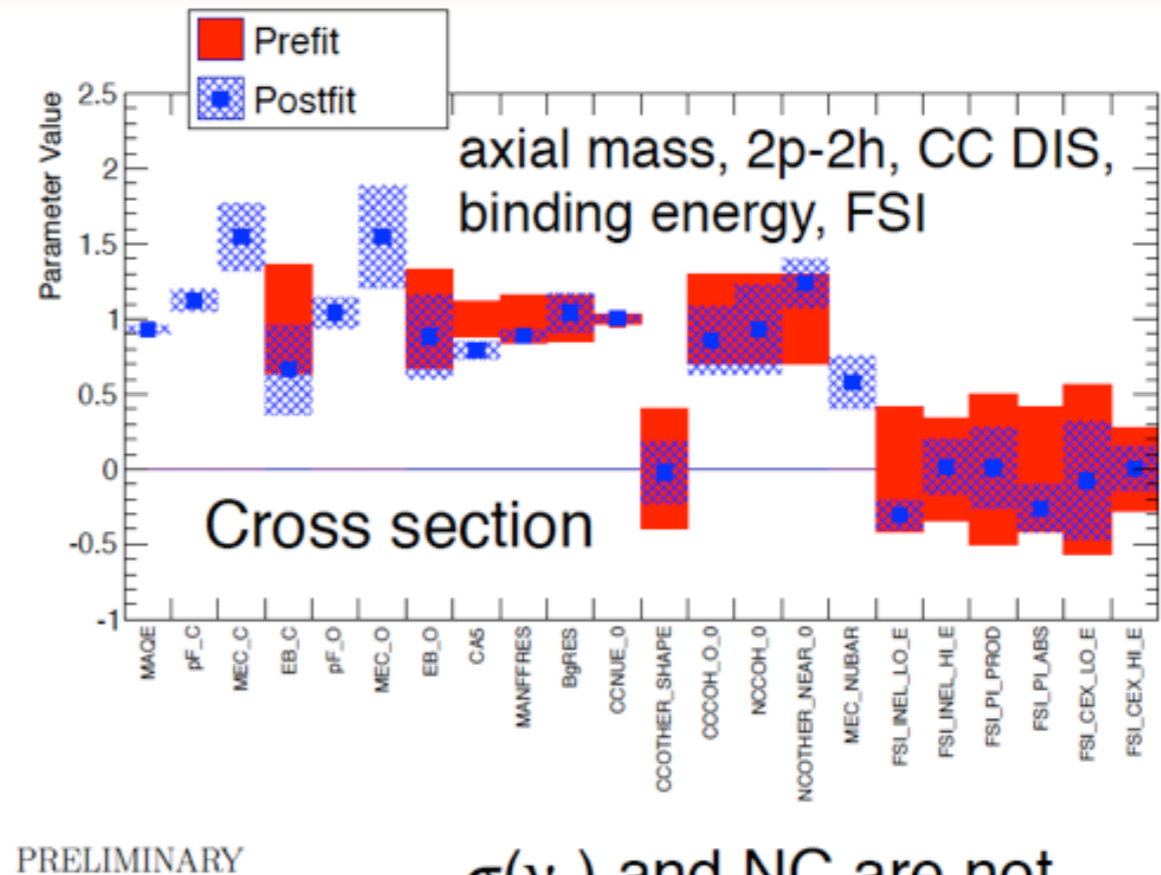
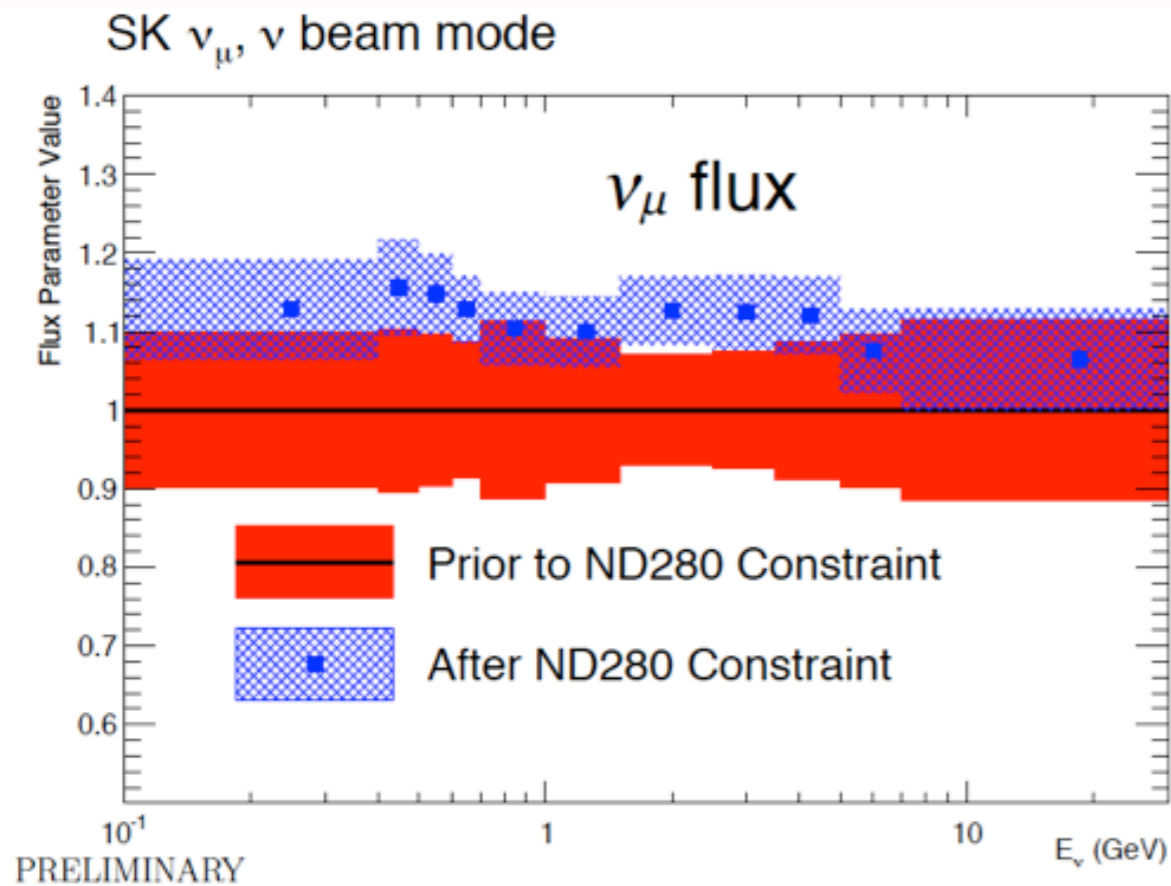
Flux Cross Section Detector Efficiency Oscillation probability

Far Detector: $N_{FD} \sim \Phi(E_\nu) \sigma(E_\nu) \epsilon_{FD} P_{osc}(E_\nu)$

Near Detector Fit: flux and cross-section uncertainties

T2K

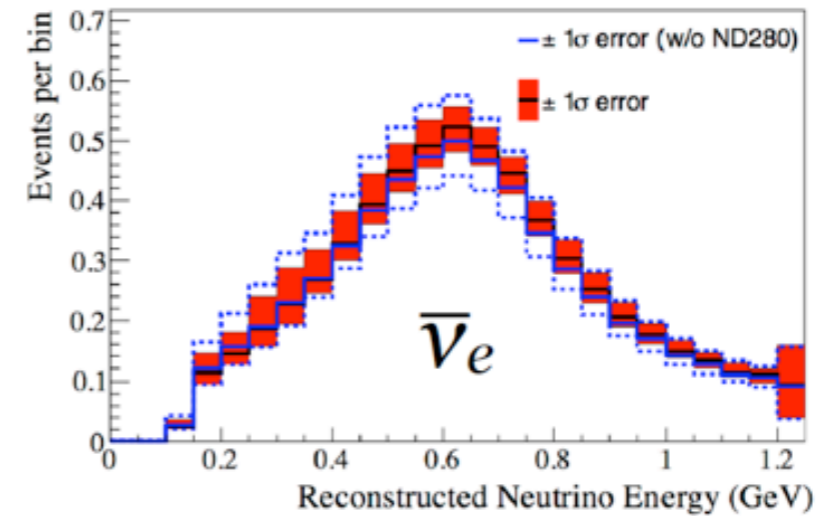
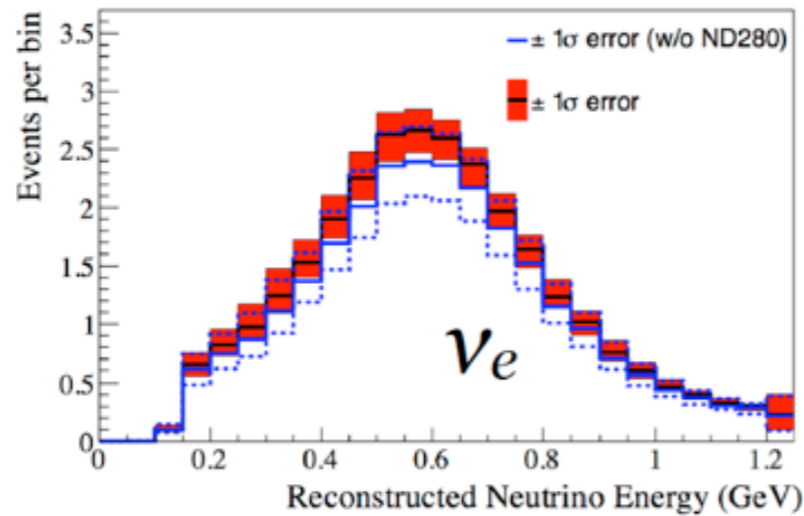
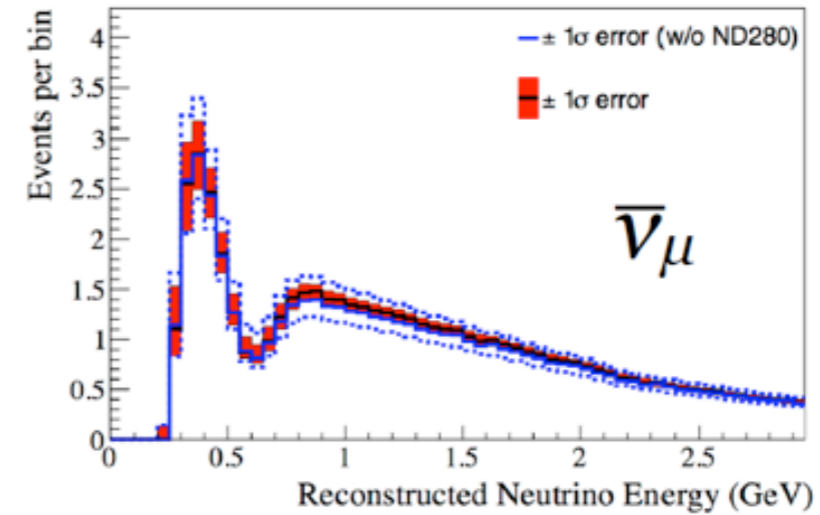
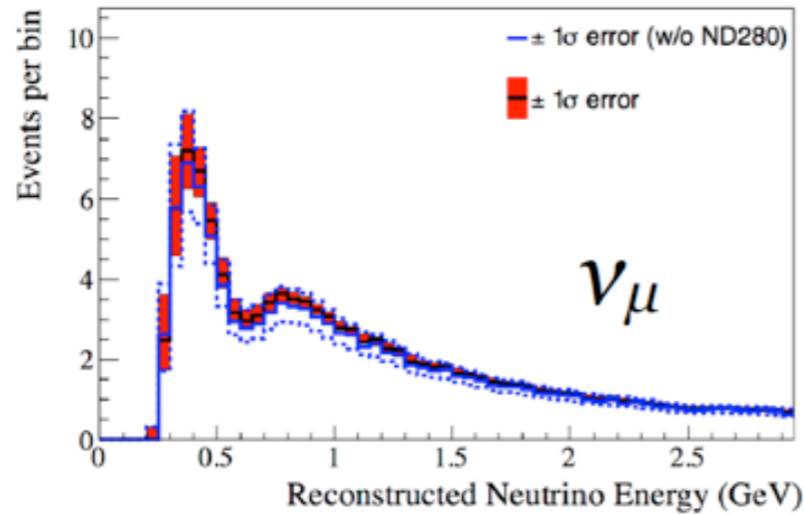
- Measure neutrino flux and cross section at ND280



$\sigma(\nu_e)$ and NC are not measured at ND280

- Flux parameters increase by $\sim 15\%$
- Cross sections \sim consistent with input value
- Flux and cross section highly anti-correlated after the data fit
- The p-value to the pre-fit prediction is acceptable (8.6%)
- Systematic uncertainties in neutrino oscillation analyses from 12-14% to 5-6%

Impact of systematic uncertainties



		Total $\delta N_{SK}/N_{SK}$	
Beam mode	sample	w/o ND280	ND280
neutrino	μ -like	12.0%	5.0%
neutrino	e-like	11.9%	5.4%
antineutrino	μ -like	12.5%	5.2%
antineutrino	e-like	13.7%	6.2%

- Improvement given by measurements with ND280 data
- Low energy: mainly NC, not measured by ND280

39

- Remember: ν_e and ν_μ phase space different in x-sec formulas + component in flux not well known

Back up

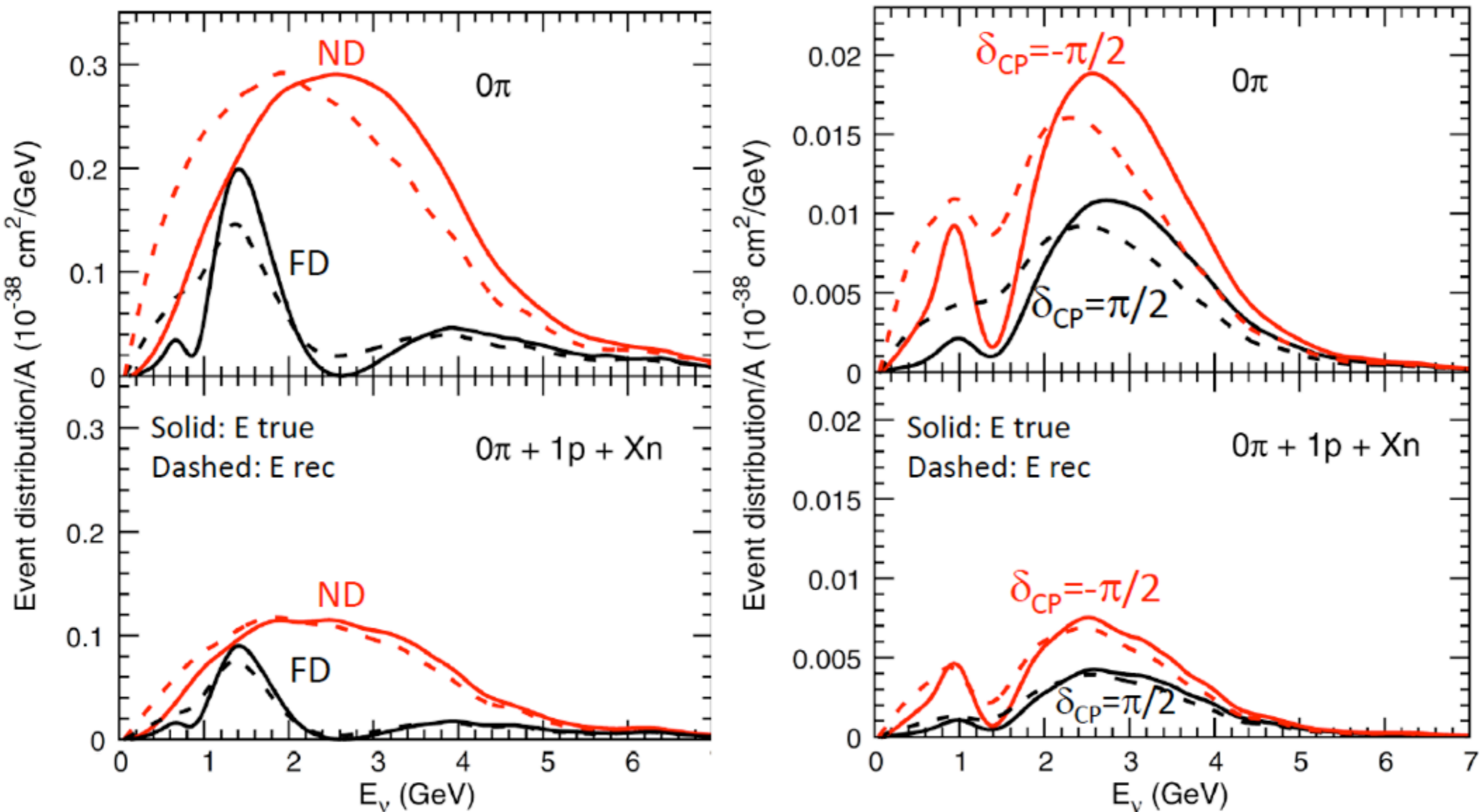


Figure 44. Left panels: distributions of charged current muon neutrino events before and after the energy reconstruction correction in the near (i.e. before oscillation) and far (i.e. after oscillation) detector. Right panels: the same for ν_e appearance CC events. Top four plots are for T2K and bottom four plots are for DUNE. The top two plots are taken from Martini *et al.* [216]. The next two plots are taken from Lalakulich *et al.* [228], and the bottom four figures are taken from Mosel *et al.* [374].

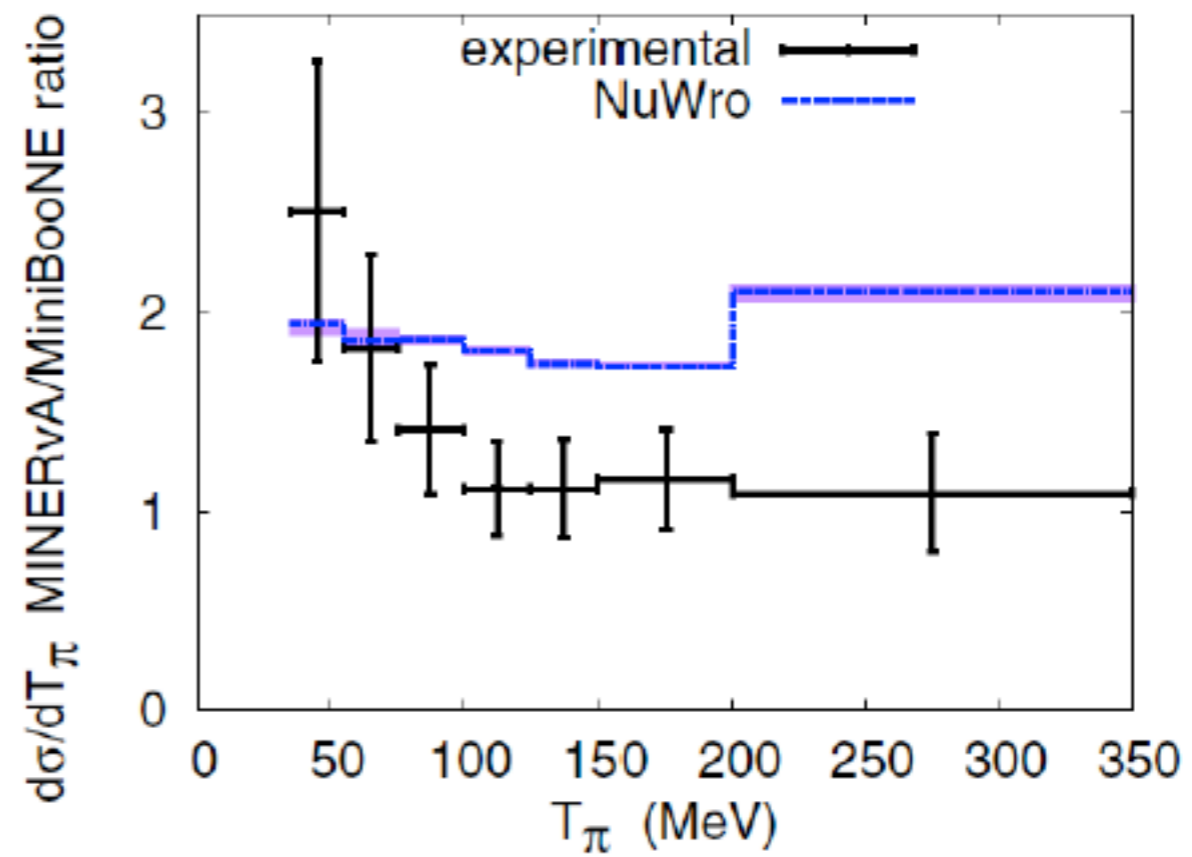
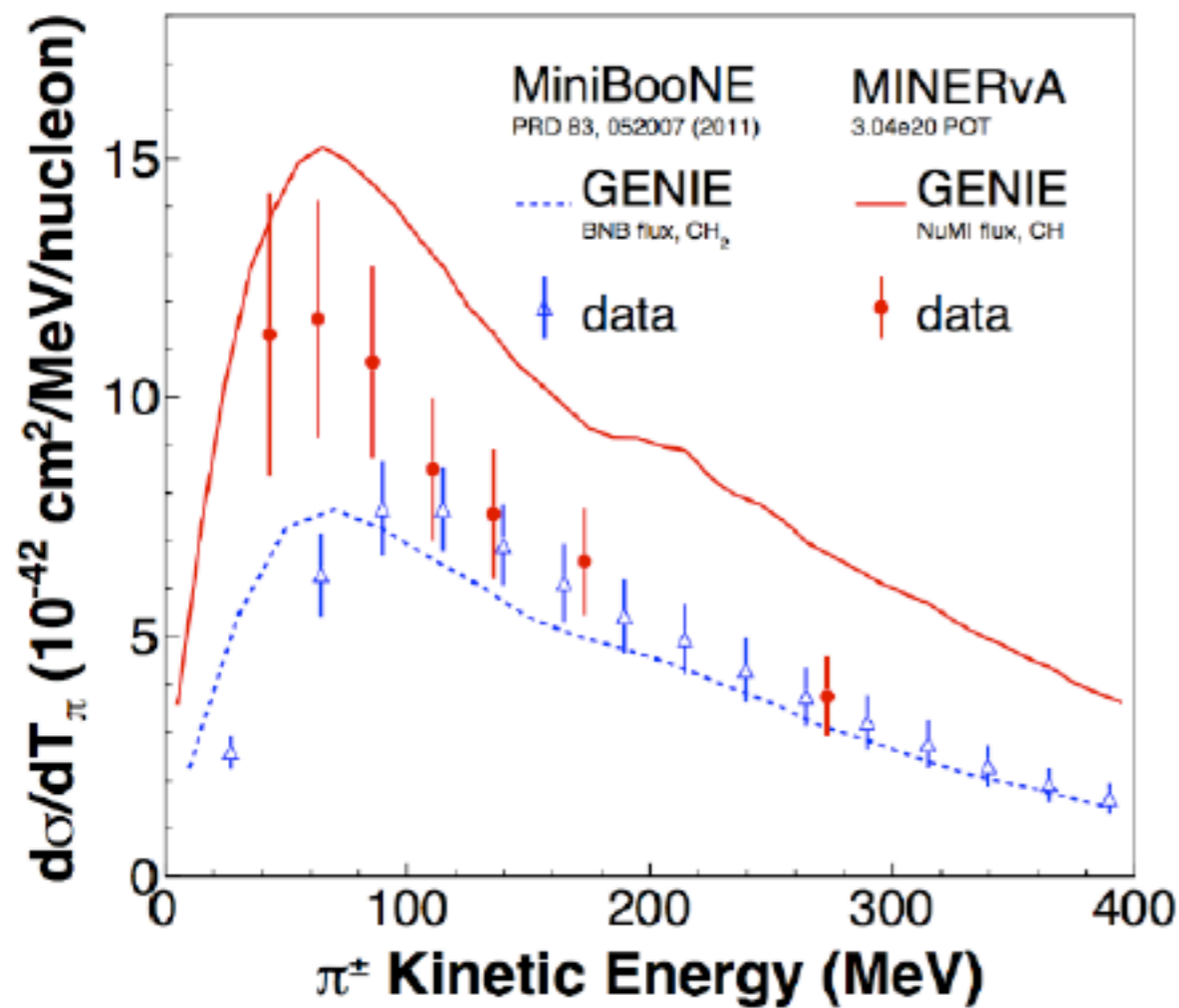


Figure 30. Flux-integrated differential cross section of charged pion kinetic energy from $CC1\pi^+$ interactions. In the left, MiniBooNE and MINERvA data are compared with GENIE prediction [115]. In the right, MINERvA to MiniBooNE data ratio is compared with the same ratio from NuWro [270].

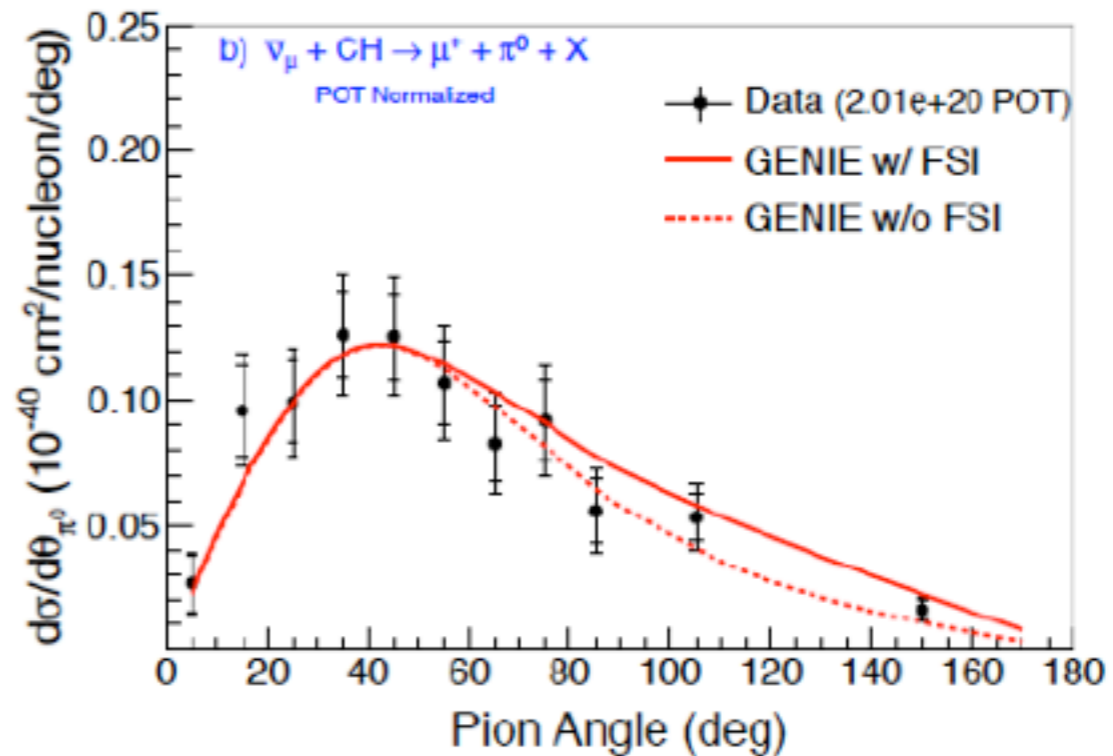
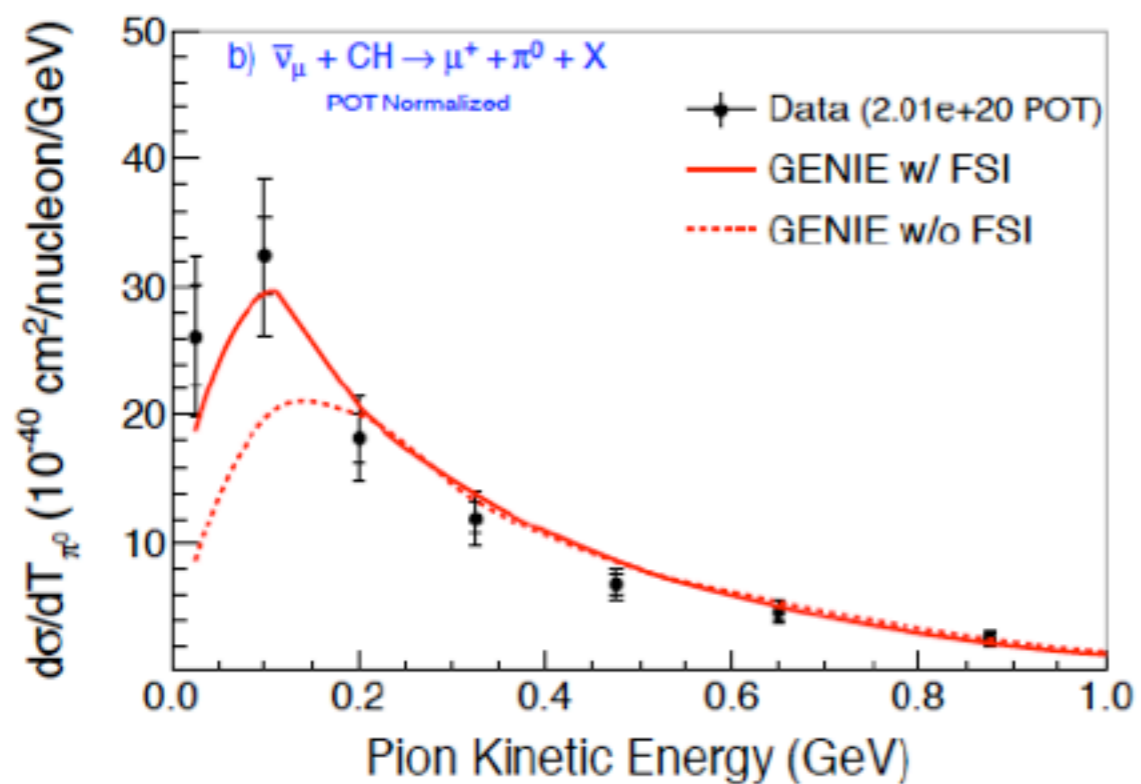
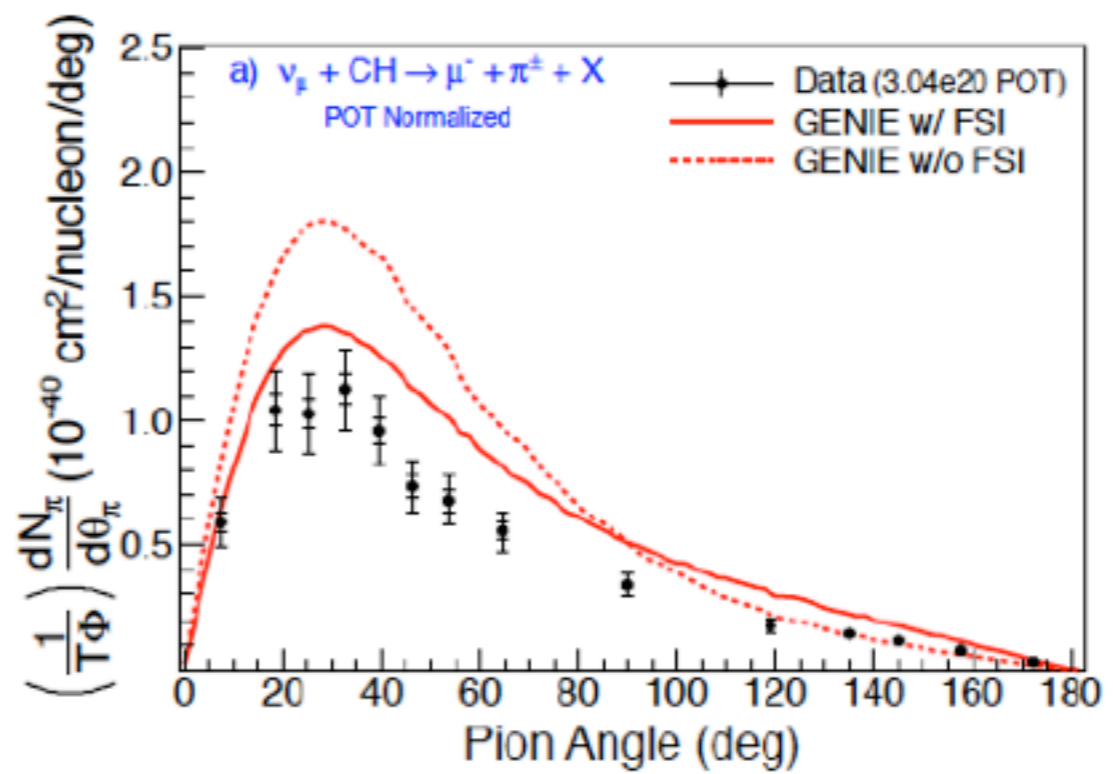
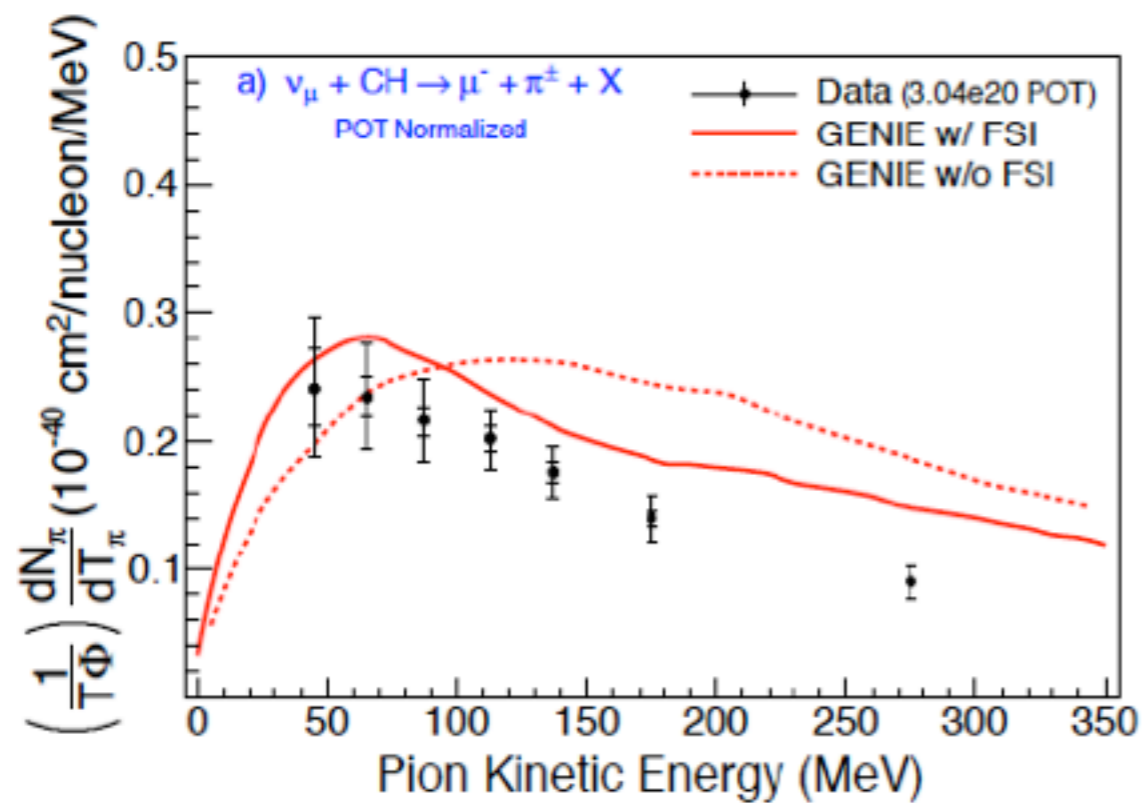
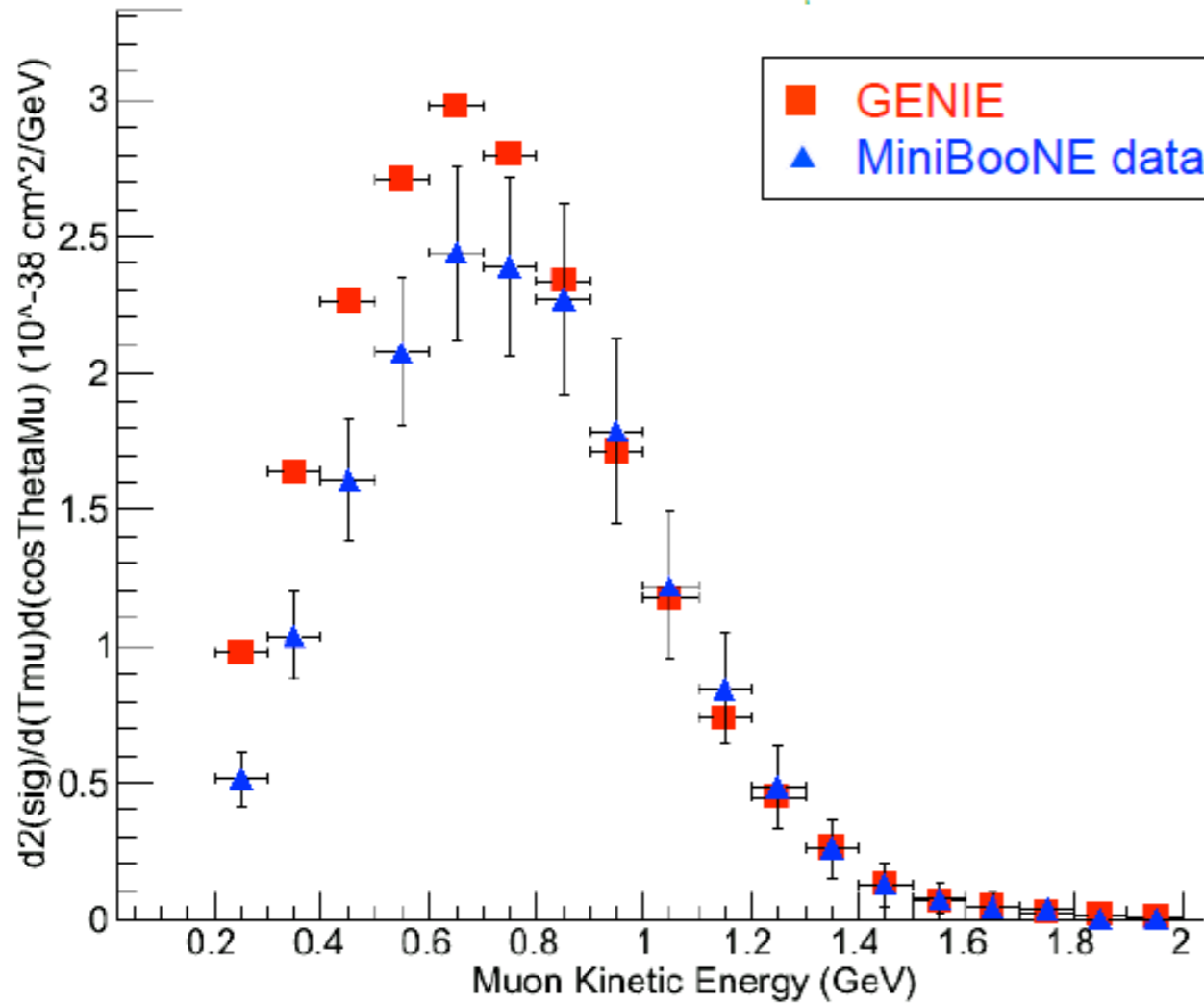
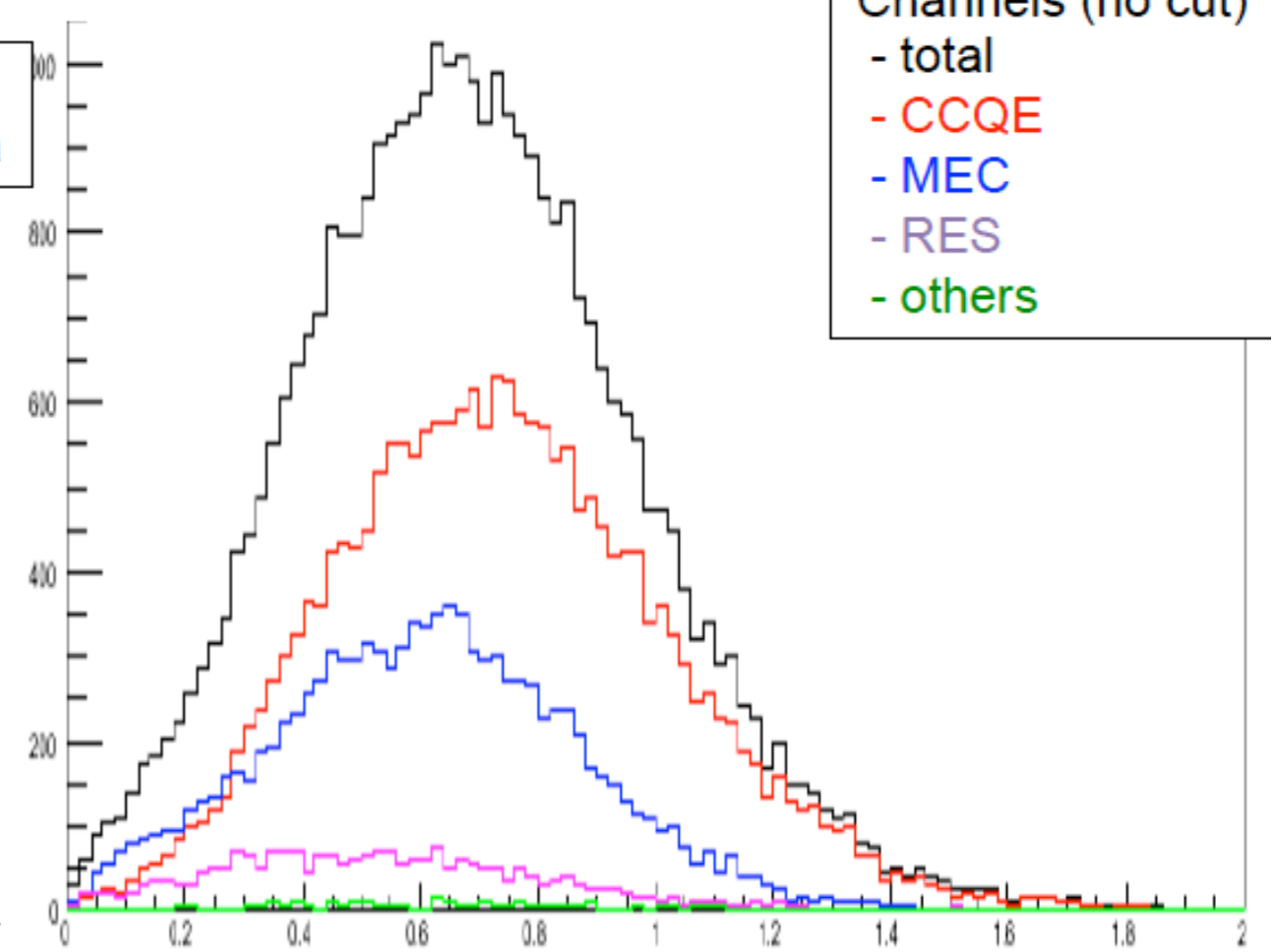


Figure 33. Neutrino $CC1\pi^+$ (top) and antineutrino $CC1\pi^0$ (bottom) production flux-integrated differential cross section, with function of π kinetic energy (left) and π scattering angle (right) [120]. Measured cross section is compared with GENIE with and without FSIs.

Comparison with MiniBooNE flux-folded ν_μ CCQE double differential cross section data
 T_{μ} distribution, $0.8 < \cos\theta_\mu < 0.9$



Decomposition of GENIE prediction
 - it shows complicated mix due to flux distribution



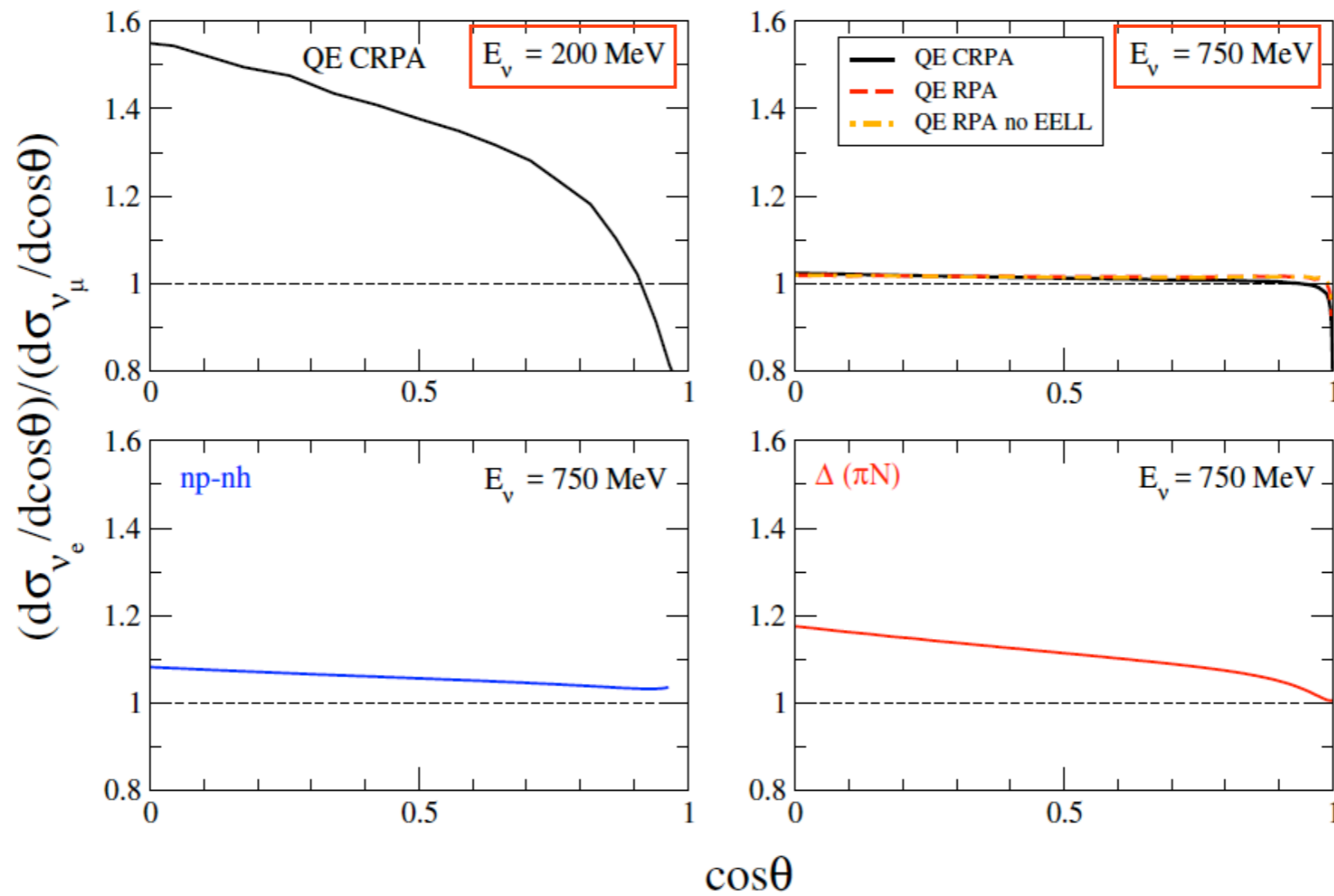


Figure 42. (color online) Ratio of the ν_e over ν_μ differential cross section on Carbon calculated for two fixed values of incident neutrino energies as a function of the cosine of the lepton scattering angle. The 1p-1h results in the CRPA approach are shown for $E_\nu=200$ MeV and $E_\nu=750$ MeV. The 1p-1h results in the RPA approach, the np-nh excitations and the one pion production (via Δ excitation) results are shown for $E_\nu=750$ MeV. The figure is taken from Ref. [219].

improving on the underlying assumptions. In comparison of various different experiments, it turns out that experiments, which rely on a relatively narrow beam spectrum and operate at energies below 1 GeV, like T2HK, are particularly sensitive to uncertainties on flavor ratios. On the other hand experiments which employ a wide beam spectrum at multi-GeV energies, like LBNE, are much less affected by these rate-only uncertainties. The imple-